ADHESION EVALUATION OF GLASS FIBER-PDMS INTERFACE BY MEANS OF MICRODROPLET TECHNIQUE

by

HABIBURRAHMAN AHMADI

B.S., Kabul University, Kabul, Afghanistan, 2006

A THESIS

submitted in partial fulfillment of the requirements for the degree

MASTER OF SCIENCE

Department of Mechanical and Nuclear Engineering
College of Engineering

KANSAS STATE UNIVERSITY
Manhattan, Kansas

2011

Approved by:

Major Professor
Dr. Kevin Lease

Copyright

Abstract

This research was intended to measure the interfacial shear strength between fiber/ matrix systems and to investigate the relation between structure-mechanical properties and performance of fiber/matrix systems. This work conducted a systematic study on model fiber/matrix systems to enhance the fundamental understanding on how variation of polymeric compositions (and hence, different structures), different curing conditions, and fiber surface treatments influence the interactions between the fiber and matrix.

In order to measure the interfacial shear strength of fiber/matrix systems, the micro-droplet technique was used. In this technique a polymer droplet was deposited on a fiber in the liquid state. Once the droplet was cured a shear force was applied to the droplet in order to detach the droplet from the fiber. The amount of the force needed to de-bond the droplet was directly related to the strength of the bonds formed between the fiber and matrix during the curing process.

In addition, the micro-droplet technique was used to evaluate effects of different crosslinker ratio of fiber/ matrix system and also to see if different curing conditions affect the interfacial shear strength of fiber/ matrix system. Surface treatment was also conducted to evaluate its effects on the interfacial shear strength of the fiber/ matrix system using micro-droplet technique.

The interfacial shear strength of fiber/ matrix system increased along with the increase of crosslinker ratio to a limiting value, and it decreased as long as the crosslinker ratio increased. Curing condition also caused the interfacial shear strength of fiber/ matrix system to increase

when it was cured at higher temperature. Fiber surface treatment exhibited a significant effect to the interfacial shear strength as well as the fiber/ matrix contact angle measurement.

Table of Contents

List of Figures

List of Tables

Acknowledgements

I am grateful to the government of my home country, Afghanistan, for this valuable offerings and funding throughout my study at Kansas State University (KSU). Special thanks to my academic advisor, Dr. Kevin Lease, for his support regarding this thesis and throughout my study at KSU and his availability to help me with my academic problems.

I am also thankful to Dr. Wang who accepted me as a research assistant and provided me financial supports for one semester before I complete my master's thesis. I would also like to thank Dr. Singh for being one of the committee members, for reviewing my thesis.

This is also the place to thank Ms. Nassim Rahmani and Ms. Elizabeth Frink, my office mates, for their technical supports throughout this research period to achieve my academic degree.

Dedication

To My Lovely Parents, To My Family Members,

To My Wife and My Son.

CHAPTER 1 - Introduction

The quest for new material development has risen during recent years. Among the new materials developed, composites have gained more popularity due to the fact their properties can essentially be tailored for various applications. Composite materials are composed of two or more chemically distinct materials with an interface separating the components.

Typically, composites are made of a continuous phase (or matrix) and a reinforcing phase. The matrix acts as the glue to support the reinforcement while the reinforcement provides the stiffness of the system. Depending on the materials used as the reinforcement and matrix, composites can be divided into several categories. One of the most common composites is the fiber reinforced polymer (FRP) based composites. In these composites the fiber, such as carbon, glass, Kevlar, or metal fiber, is embedded in the polymer resin. This combination has the low density and high strength of the fiber yet the toughness of the polymer matrix, provided that the design and fabrication of the components are carried out correctly. The desirable chemical and mechanical properties of the composite are, however, dependent of the interface formed between the fiber and matrix. The interface illustrated in Figure 1.1 is at the fiber/matrix boundary where the stress transfer between the polymer matrix and the fiber occurs. This interface has unique properties that are different from the properties of either the fiber or the matrix. It has been shown that the performance of composites can be directly related to the strength of the bonds formed at the interface region. Therefore, studying and understanding the relation between chemistry and interfacial properties of composites can open new avenues for tailoring, in a more direct manner, the adhesion properties and performance of these materials for engineering

applications. It has been shown that for any fiber/matrix system, the interfacial strength is significantly influenced by the fiber surface treatment and matrix composition [1-4].

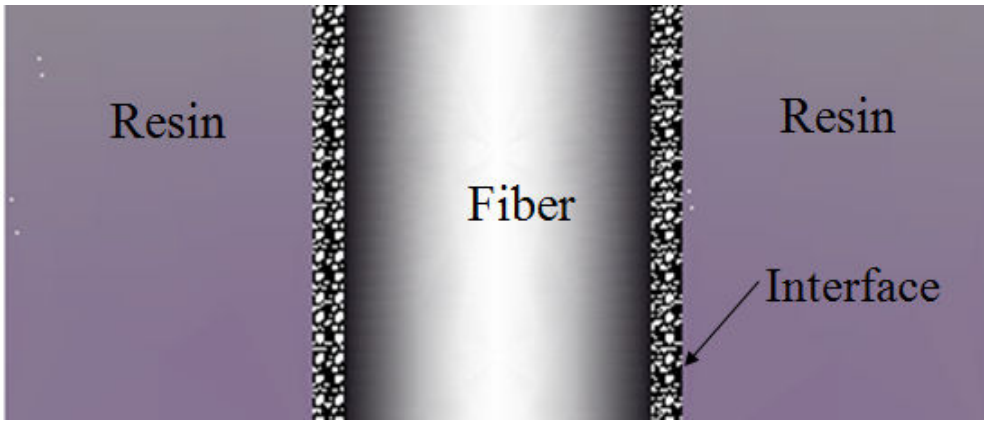

Figure 1.1 Illustration of the interface region in FRP

A need for a simple, yet accurate method that can be used in characterizing the interface properties of FRP composite materials has led to the development of micromechanical experimental techniques. Such techniques include fiber pull-out, fiber push-out, fiber fragmentation, and micro-droplet tests. These techniques utilize small amounts of materials to determine the adhesion properties of the fiber/matrix system.

The objective of this study is to develop a micro-droplet (or micro-bond) test device and then use the device to investigate the level of adhesion involved in the interfacial region of model glass fiber/polymer systems in a systematic manner. Bare smooth borosilicate glass rods, referred to as glass fibers, are used in conjunction with a mechanically well-characterized polymer, polydimethylsiloxane (PDMS), to study the adhesion behavior of the system as a function of different polymeric compositions (and hence, different structures), different curing conditions, and some fiber surface treatments. The ability to determine the adhesion of model systems and link chemical properties of the interface to mechanical properties of the composite provides a

better fundamental understanding of several issues that control the composite performance including polymer chemistry, fiber surface treatment (e.g. specific functional groups or contaminants), and impact of the interface region on the strength and durability of the system. The results of this research will shed light on the feasibility of using the micro-droplet test technique in evaluation of more complex fiber/matrix systems or specific applications.

The goals of this research are as following:

1. Develop and set up the micro-droplet experimental apparatus to measure the adhesion between fiber/matrix systems
2. Investigate the interfacial properties of model fiber/matrix systems and study the impact of possible polymer compositions, curing conditions, and fiber surface treatment on the interface strength

This thesis is organized in the following form:

Chapter 2 provides an overview of the micromechanical techniques used to evaluate the adhesion of fiber/matrix systems.

Chapter 3 introduces the experimental setup fabricated and used in this research along with the experimental procedure.

Chapter 4 describes the materials which are tested in this study and goes over the description of specimen preparation and test evaluation.

Chapter 5 details the methods used for the PDMS crosslinking ratio and discusses their results.

Chapter 6 describes the effects of different PDMS droplet curing conditions with results and discussion.

Chapter 7 evaluates the effects of fiber surface treatment on the glass fiber/PDMS interface and shows the results with discussion.

Chapter 8 summarizes the entire study with conclusions.

CHAPTER 2 - Micromechanical Techniques

In this chapter, the experimental micromechanical techniques that are typically used for measuring the adhesion of fiber reinforced polymer based composites are described. These techniques include fiber pull-out test, fiber push-out test, single fiber fragmentation test, and micro-droplet test. All of these approaches are exploited to evaluate the mechanical properties of composites as well as to investigate the influence of chemical composition of the polymer matrix and the effect of fiber surface treatment on the composite performance. Despite this, the results obtained by one technique cannot typically be compared to another technique. Therefore, the results of a given technique are typically used in a comparative manner for a given material system and while systematically changing one or more variables in the material system (matrix chemistry changes, fiber surface treatments, curing procedures, etc).

As stated earlier, the focus of this study was the development and usage of a micro-droplet test; therefore, this technique will be covered in detail in the next chapter while all techniques will be reviewed briefly in this chapter for comparison purposes.

Fiber Pull-out Test

Figure 2.1 shows a schematic view of the fiber pull-out test. In this technique one end of the fiber is embedded in the polymer resin and the free end is loaded in tension while the matrix is fixed in place. Here, the maximum load required to pull the fiber out of the matrix block is recorded as a function of the embedded length. The interfacial shear strength (τ_{IFSS}) can be calculated according to the following equation:

$$\tau_{IFSS} = \frac{F_{\max}}{\pi d_f L_e} \tag{2.1}$$

where F_{max} is the maximum force, d_f is the fiber diameter, and L_e is the embedded length of the droplet.

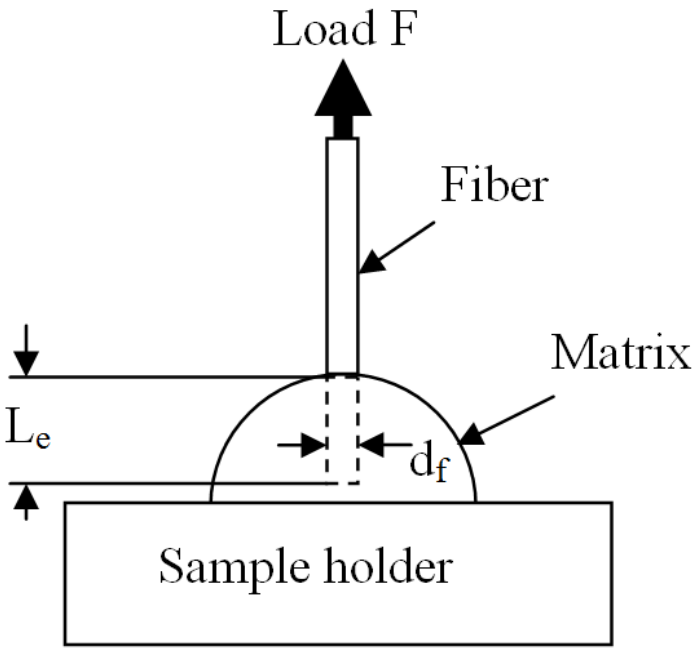

Figure 2.1 Schematic of fiber pull-out test

In this technique the fiber alignment plays a significant role in the accuracy of the test [5]. Another limitation that is associated with this technique is the embedded length of the fiber in the resin. If the fiber is embedded too far in the matrix, the applied force will not be able to break the bonds between the fiber/matrix systems; the fiber will fracture instead. This problem, however, can be resolved by making the resin block smaller.

Fiber Push-out Test

Similar to the pull-out method, in this test a single filament is embedded in the matrix in the fiber push out technique. However, the fiber in the push-out method is loaded in compression by a hard tip. During the test, a force-displacement curve is provided to monitor the displacement

of the tip. The maximum force from the curve was used to calculate the interfacial shear strength of the system. The interfacial shear strength can be calculated from equation (2.1).

In this technique, the fiber has to be hard enough to be pushed out of the polymeric resin. Glass and metal fibers are appropriate fibers for this method whereas polymeric fibers cannot be used in this method because they are not hard enough to resist splitting due to the diamond tip [6].

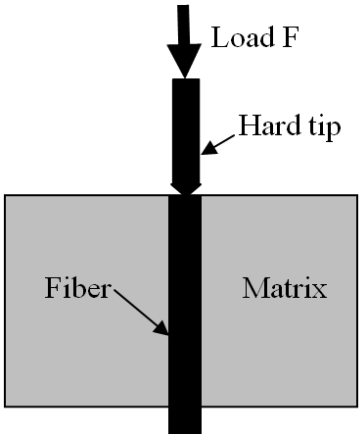

Figure 2.2 Schematic of single fiber push-out test.

Single Fiber Fragmentation Test

Another technique to evaluate the adhesion of fiber/matrix systems is the single fiber fragmentation test. In the single fiber fragmentation test a single fiber is embedded in a dog-bone shaped resin specimen, illustrated in Figure 2.3. The fiber is aligned along the center of the specimen and the dog-bone specimen is loaded in tension in the axial direction. Once the specimen is stretched, tensile stress transferred from the resin to the fiber through shear stress at the interface builds up until the fiber breaks into lengths (See Figure 2.3 (b)) [7]. The test then continues until saturation occurs. At saturation an applied stress to the specimen can no longer produce a large enough stress in the fiber to reach its breaking stress. The fiber-break lengths at

saturation are measured afterwards and averaged. The critical length (l_c), which is obtained from the fragmentation data, is used to determine the interfacial shear strength as following:

$$\tau_{IFSS} = \frac{\sigma_f}{2}\frac{d_f}{l_c} \tag{2.2}$$

where σ_f is the ultimate strength of the fiber

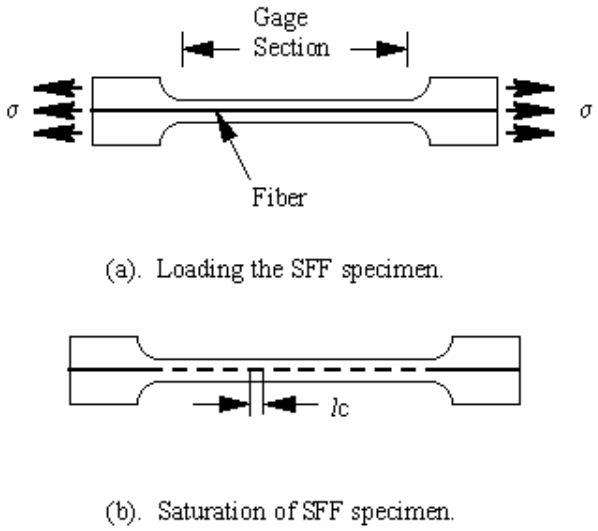

Figure 2.3 Schematic of single fiber fragmentation test [7]

Micro-Droplet Test

The micro-droplet technique is a modified version of the fiber pull-out test where the amount of the polymer matrix is decreased. This technique was first developed by Miller [8]. In the micro-droplet test a small droplet of the polymer in the liquid state is deposited on a fiber. Once the droplet is cured, a shear force applied by a micro vise detaches the droplet from the fiber. The maximum force required to detach the droplet is a measure of the shear stress in the interface region of the polymer/fiber system. The system arrangement is depicted in Figure 2.4. Similar to the fiber pull-out test, the interfacial shear strength is determined from equation (2.1).

The micro-droplet test can potentially provide fiber/matrix adhesion strength as well as the frictional data after the interfacial bond is broken. This technique can be used for any fiber/matrix system, regardless of the fiber size, based on the strength of the fiber. Studies [8, 9] have shown that a larger embedded length or embedded area due to variation of droplet size decreases the interfacial shear strength.

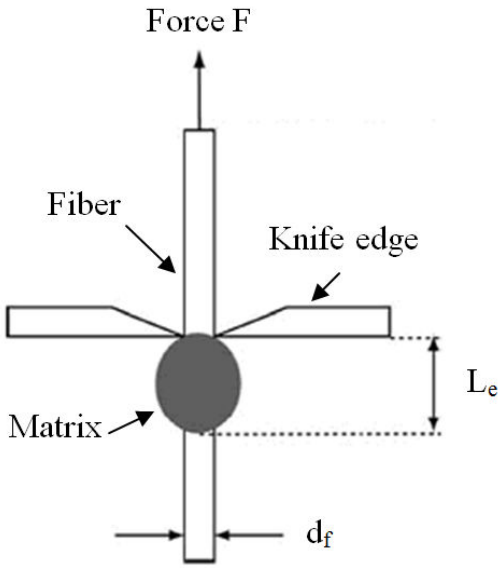

Figure 2.4 Schematic of micro-droplet test

There are many other modified micro-droplet testing methods such as quasi-disk type micro-droplet and hemispherical micro-droplet that have been described elsewhere [10]. Table 2.1 shows a comparison of different micromechanical characterizing testing techniques. The differences are mostly related to the fiber/matrix types, different surface treatments, and curing conditions rather than testing methods.

This was a brief discussion of a variety of micromechanical methods, but the technique chosen for this study (micro-droplet technique), along with the developed setup for this technique will be discussed in-depth in the next chapter. Chapter 4 will then be focused on the

description of the materials that have been used in this study and the techniques for the specimen preparation.

Table 2.1 Comparison of different testing techniques

Fiber/resin system	Technique	Average interfacial shear strength (MPa)	Reference
Cellulose/Polystyrene	Fragmentation	13	Trejo-O'Reilly [11]
T-300/Epicote 828	Fragmentation	52.4	Wada Et al [12]
Carbon fiber/YD-128	Hemi-spherical	38.1	Choi Et al [10]
Boron/EDT-10 epoxy	Micro-droplet	88.2	Zhandarov [9]
Carbon fiber/AER-250	Micro-droplet	55.3	Kang Et al [13]
Carbon fiber/YD-128	Micro-droplet	32.7	Park Et al [14]
Carbon/YD-128 epoxy	Micro-droplet	33.7	Choi Et al [10]
Celion/Epon 828	Micro-droplet	65.3	Guar and Millar [15]
Cellulose/ Polystyrene	Micro-droplet	2.7	Trejo-O'Reilly [11]
E-glass/Epon 828	Micro-droplet	43.5	Guar and Miller [15]
E-glass/EPON 828	Micro-droplet	33.1	Miller Et al [8]
E-glass/TEGDMA	Micro-droplet	33.8	McDonough Et al [2]
Flax/PP	Micro-droplet	3.39	Czigany Et al [16]
Hemp/PP	Micro-droplet	5.07	Czigany Et al [16]
Henequen/UPE	Micro-droplet	5.5	Cho Et al [17]
Kevlar 29/Epon828	Micro-droplet	40	Guar and Miller [15]
Kevlar 49/Epon828	Micro-droplet	41.4	Guar and Miller [15]
M5/D.E.R 355	Micro-droplet	58	Leal Et al [18]
Sisal/PP	Micro-droplet	4.6	Czigany Et al [16]
Steel wire/EDT=10 epoxy	Micro-droplet	74.2	Zhandarov [9]
T-300/Epicote 828	Micro-droplet	48	Wada Et al [12]
T-300/Epon 828	Micro-droplet	18.5	Biro Et al [3]
Carbon fiber/Polystyrene	Pull-out	24	Li et al [5]
Glass/PP	Pull-out	135	Zhandarov [9]
Carbon/ YD-128	Quasi-disk type	20	Choi Et al [10]

CHAPTER 3 - Overview and Experimental Method

In this chapter, a comprehensive overview of the micro-droplet test setups will be discussed. This also includes discussion on variations of test setups, the advantages and disadvantages of each, and which setup has been used in this study. Our developed micro-droplet apparatus will be described in detail. Explanation of the experimental testing procedure for this study is also another important part of this chapter.

Overview of Micro-Droplet Technique

As has been mentioned previously, the goal of this study is to develop a micro-droplet testing device. Therefore, the micro-droplet method will be illustrated in-depth here, including setup and the test procedure.

The micro-droplet technique has a variety of uses in aerospace engineering, transportation, and military applications, and it is much simpler than the micro-pullout technique because it can handle with smaller fiber sizes and easy to build smaller embedded length to prevent fiber fracture. Therefore, it is a more applicable testing method in the study of interfaces compared to other methods, and it is an easy tool to determine fiber-matrix frictional properties [1] which is not included in this study. In comparison with other methods, the micro-droplet technique consistently gives a higher value of interfacial shear strength because of its smaller embedded area that can be tested [15].

As discussed earlier, the interfacial shear strength can be calculated by equation (2.1). In this equation, the stress is considered as uniformly distributed along the embedded area of the droplet [8], but there are some other factors that can contribute to the variation of the τ_{IFSS}. For example, the geometry of the droplet has an influence on the τ_{IFSS}, as the residual stress will increase with

the increase of interfacial edge angle (the angle the end of the droplet makes with the fiber). This means that the τ_{IFSS} of a droplet with a spherical shape is higher than that with an elliptical shape (with all other things being the same). This study was performed by Cen et al [19] using Micro-Raman spectroscopy technique. The frictional stress, residual thermal stress, and crack propagation are other factors that can participate in the variation of the interfacial shear strength [9]. The debonding force vs. embedded length in much research shows that the debonding force is proportionally related to the embedded length until the fiber fractures. When the fiber breaks, the embedded length is called the critical length, and the debonding force and embedded length are no longer proportional to each other [14].

Studies show [8, 20] that there are three different general trends for shear force vs. displacement profiles from recorded data during debonding. In the first case, when actual shear occurs, the force may rise gradually to a peak and then it suddenly drops to a frictional force (see Figure 3.1-a). In a second case, the force may gradually reach the maximum and decreases gradually to a frictional force, higher than the frictional force seen in the first case (see Figure 3.1-b). Alternatively, if the droplet slips through some flaws, the force does not reach the maximum with one slope – during slip the slope decreases. The decrease from the peak may occur gradually or as a sudden drop in this case, and the frictional force maintained after the drop may vary around the frictional forces in the first two cases (see Figure 3.1-c).

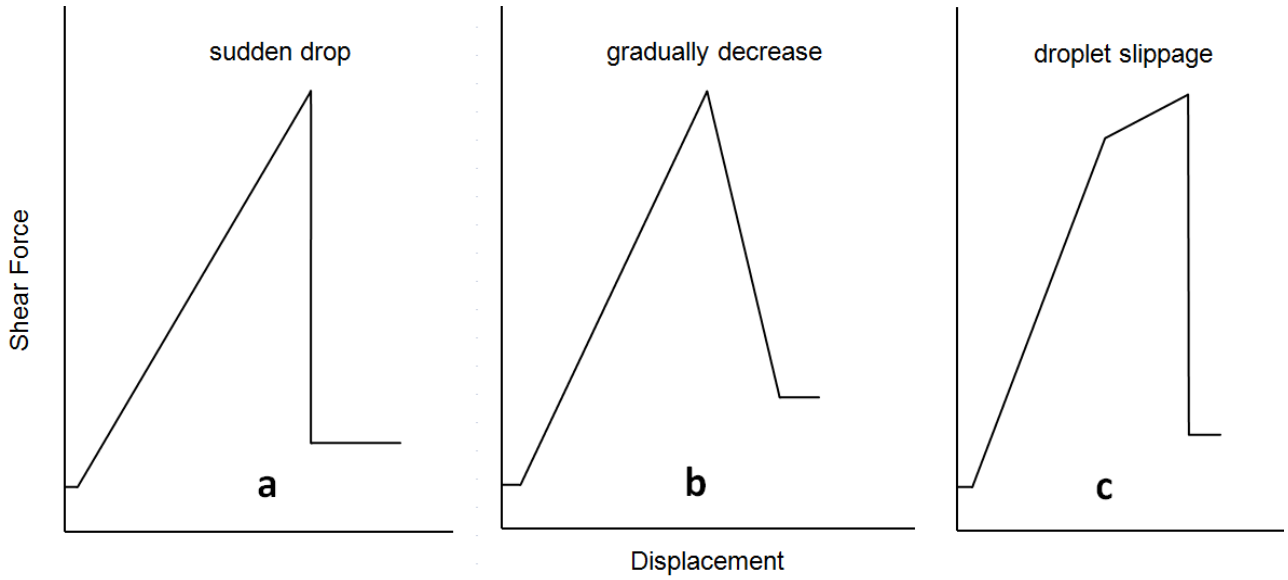

Figure 3.1 Three general trends of shear debonding [modified from 8, 20]

Many different variations to the micro-droplet apparatus have been developed, including orientation of the apparatus (horizontal or vertical) and moving part (micro-vises or load cell). For a vertically installed apparatus, the fiber is mounted on a tab connected to a load cell, and the other end of the fiber is free. The load cell can either pull the fiber upward by keeping the droplet motionless in contact with the micro-vises, or the micro-vises can pull the droplet downward [1-3, 6, 8, 13-15, 18, 21]. Figure 3.2 shows a schematic of vertically installed micro-droplet setup.

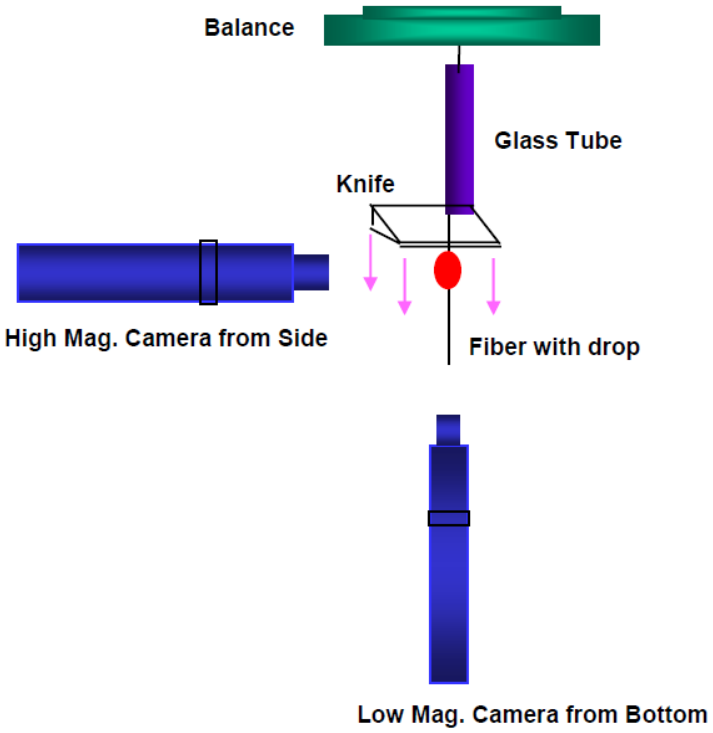

Figure 3.2 Schematic of a vertically installed micro-droplet setup (only one knife edge is shown) [6].

For a horizontally installed setup, there are different ways to mount the specimen. If both ends of the fiber are glued, one end fixed to a tab and other end fixed to a load cell, one end of fiber should be pulled by the load cell, and the knife-edges should be closely contacting the droplet before running the test. Another technique is to fix one end of the fiber to the load cell by a tab and leave other end free; then, the test can be run by either pulling one end of the fiber by a load cell or pulling the droplet by micro-vises to the opposite direction [19, 20, 22-25]. Figure 3.3 shows a schematic of a horizontally installed micro-droplet test setup with one end glued.

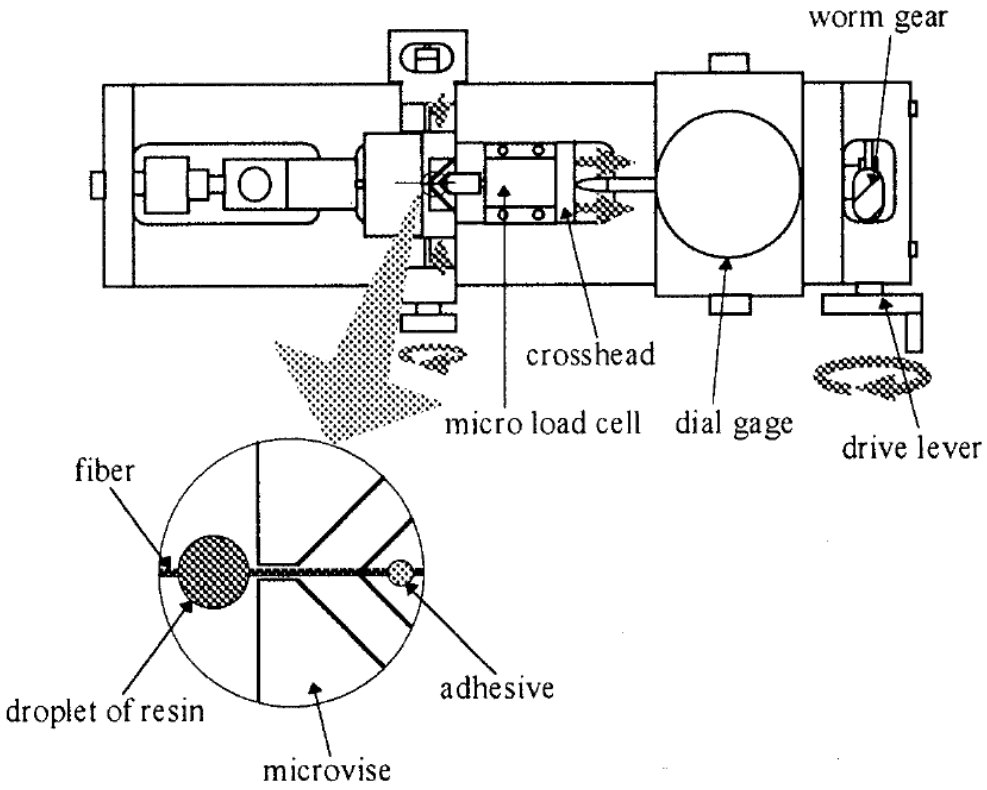

Figure 3.3 A schematic of horizontally installed micro-droplet setup [12].

All of these techniques are applicable in interface studies and have their own advantages and disadvantages. For example, to study surface moisture effects, the vertically installed setup is a good tool [14], but if we want to study the geometry effects on the τ_{IFSS}, using a horizontally installed setup is a best tool [19]. This orientation allows the easiest placement of cameras for observation of the geometrical changes during the test. The next section of this chapter illustrates the experimental setup that has been developed in this research.

Experimental Apparatus

Figure 3.4 shows a schematic view of the micro-droplet test setup developed for the present study. In this setup one end of the fiber is glued to a metal tab that is connected to a 1N load cell (ULC-1N Interface®). The other end of the fiber is free, yet supported by another tab to

prevent the free end from bending or displacing during the test. Two knife edges, perpendicular to the fiber, are attached to two independent manual translation stages which are used to adjust the position of the knives with respect to the fiber and droplet (in the perpendicular direction) before each test is started. During the test, the forward motion of these knife edges is linked and driven by a computer-controlled translation stage (M-111.2DG from PI®) to shear off the droplet. An LVDT is used to obtain the displacement of this translation stage (the displacement of the droplet in the force-displacement curve). To adjust the location of either ends of the fiber or the computer-controlled stage, three linear stages are used. The whole setup is located on a bench plate with self-adjusting leveling feet.

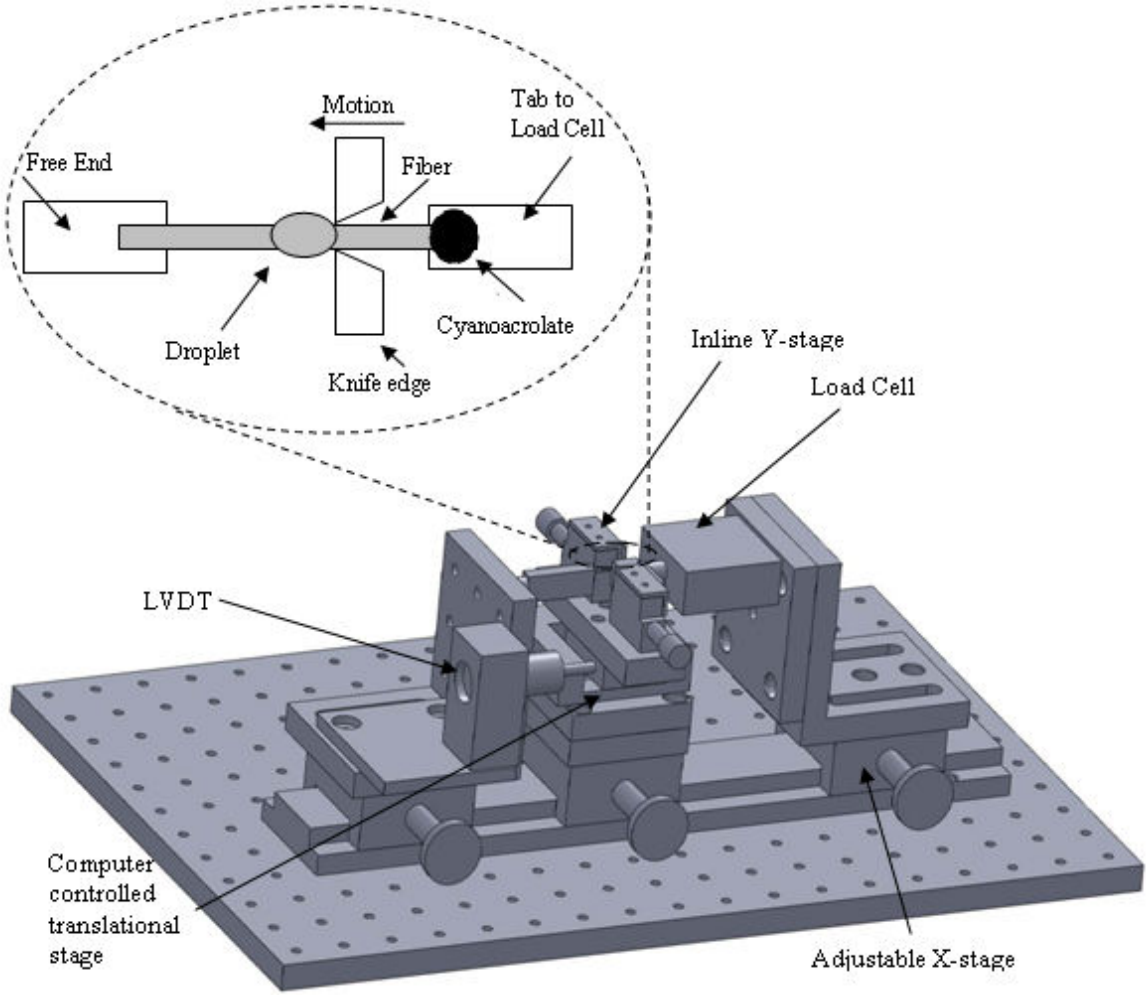

Figure 3.4 Schematic of the micro-droplet test set-up

Load Cell

The shear force to detach the PDMS micro-droplet from glass fiber in this experiment is less than 1N, so a load cell with a sufficient resolution to measure the shear force is needed in this experiment. A 1N load cell (ULC-1N Interface®) with a maximum reading error of ±%0.05, operating temperature range of -55 to 90 ºC, safe axial overload of ± %1000, and safe side overload and axis moment of ±%500 was used to fulfill this need.

The load cell was hooked to a digital meter (Interface®) which was connected to a transducer electronic data sheet (TEDS) to transfer the data to the host computer trough an RS-232 serial port using a program written in MATLAB to record the shear force data points from the experiment with the motor rotational signal. The compatibility of the TEDS with the load cell was calibrated by its supplier (Interface®), which shows a measurement uncertainty of 0.04% in the output data recorded in mV/V, is presented in Appendix A. In addition, the load cell was calibrated in the laboratory by using standard weights of 10-180mg. These weights were first measured by a high resolution balance (Explore Pro analytical balance from OHAUS), and then compared with the load cell (shown in Appendix A). The calibration data shows that there is no significant difference in the calibration. About 4-35% of the maximum range of the load cell was used to measure the interfacial force in the micro-droplet test experiment which is a large enough amount for this load cell. The maximum force from this record was used to calculate the interfacial shear strength of the glass fiber/PDMS droplets.

Spring Loaded LVDT Position Sensor

A GSA 750-200 LVDT position sensor from MACROSENSORS was used to measure the displacement of the micro-translation motor. The nominal displacement range of the LVDT was ±5.0 mm with a linearity error of +/-0.5%. It was programmed by MATLAB to transfer data points to the computer by using an RS-232 serial port. The recorded data from LVDT was compared to the displacement of the micro-translation motor, and displacement of the micro-translation motor was used as the displacement of the specimen to create load vs. displacement plot.

Micro-Translation Motor

Since the crosshead speed of the sliding micro-vises is also important in this micro-droplet study, a computer-controlled micro translation stage (M-111.2DG from PI®) was used to control the motion of the micro-vises along the fiber direction. The micro-stage's motion was controlled by its accompanied interface software (PI-MikroMove(R)). The controlled crosshead speed was 0.002 mm/sec, which will be discussed later. Furthermore, the rotational signal of the micro-translation motor was used as the displacement of the micro-droplet specimen. This micro-translation stage had a travel range of 15 mm, with a motor resolution of 0.0086 μm. The motor could be controlled with a maximum velocity of 2 mm/second. The maximum safe load for the motor was designed up to 30 N, and it could be run with a maximum push/pull and lateral force of up to 10 N. The operating temperature for the motor was limited from -20 to +65 C.

Microscope and Digital Camera

The geometry of the micro-droplet specimens were measured by using a SZH10 stereoscopic microscope from Olympus with a magnification of up to 140X, and the magnified geometry of the micro-droplet specimens were transferred to the computer by a digital camera from Spot Insight. The camera was mounted on the top of the microscope. The fiber diameter and embedded length of the droplet were measured by accompanied software (Advanced Spot) of the camera supplier.

Experimental Procedure

The prepared micro-droplet specimen, which will be illustrated in Chapter 4, was placed on the tabs as shown in the inset of Figure 3.4. One end of the fiber was glued on the tab attached to the 1N load cell, and the other end of the fiber was left free but supported by the second tab to

avoid bending the fiber. A shear force was applied to the droplet by means of two knife edges perpendicular to the fiber surface. These knife edges were moved by a computer-controlled micro translation stage (M-111.2DG from PI®), illustrated in a previews section, at a constant crosshead speed. The crosshead speed for all experiments was maintained at 0.002 mm/sec. For comparison purposes, the crosshead speed in other studies [1, 3, 8, 13-15, 20, 22] ranged from 0.001mm/s to 0.0167mm/s. Therefore, a smaller speed was used in this experiment to better control the displacement. The load profile was also recorded for each experiment using the method which is illustrated previously. The fiber diameter and the embedded length of the droplet were measured prior to each experiment using a stereoscopic microscope as was described earlier. The peak load along with the fiber diameter and embedded length can be used later to determine the interfacial shear strength of the system.

The next chapter will discuss the material used in this study and the techniques used to prepare and treat the specimens.

CHAPTER 4 - Test Materials and Specimen Preparation and Evaluation

In this chapter, a full description of the material and specimen preparation processes used on the glass fiber and PDMS polymer will be provided. The processing parameters (1) crosslinking ratio, (2) curing condition, and (3) fiber surface treatment were systematically evaluated in this study. Basic material/specimen preparation processes will be discussed in this chapter. Details of the variations in the selected processing parameters will be discussed in subsequent later chapters.

Material Selection

As mentioned earlier, the micro-droplet method is well suited to the characterization of composite materials, especially polymeric adhesives with reinforced fibers. Therefore, glass fiber (bare smooth glass rod) and (PDMS) were selected as reinforced fiber and adhesive, respectively, to characterize their interfacial properties; however, the use of PDMS as the droplet in the micro-droplet test has not been stated in the published literature. The reason to choose glass rod and PDMS as reinforced fiber and matrix in this study is to observe their applicability in the micro-droplet system. Furthermore, we wanted to prove that glass rods can be used as alternative reinforced fibers instead of wood fibers in wood adhesives because it is hard to produce wood fibers in small sizes, and the surface of wood fibers is not as smooth as glass rods.

Glass Fiber (Rod)

Borosilicate glass fibers, with diameters ranging from 80-200 μm, were used in this study. The fibers weren't commercially treated or branded fibers. The glass fibers were

professionally prepared by a glassmaker in the Chemistry Department of Kansas State University by heating the glass rod and then pulling the rod ends in opposite directions until a uniform, desired diameter rod was achieved.

PDMS

A two-part elastomeric kit PDMS (Sylgard 184, Dow Corning) was used in this study. This kit contains two components: one is the silicone elastomeric base and the other is a curing agent (crosslinker). Both of these components are in liquid form. The mixing ratio and preparation procedure will be described in later sections. PDMS is a silicon-based organic polymer that has a repeating unit of silicon and oxygen in its structure. Although PDMS has not been investigated using the micro-droplet technique, it was selected for characterization of its interfacial properties with glass fiber because it acts as a viscous liquid at high temperature and has a smooth surface to make a uniform and unshrinking surface for a micro-droplet. PDMS is incompressible and has a constant surface energy. Its modulus typically varies from 100 kPa to 3 MPa depending on different curing conditions.

Material Preparation

The material preparation process for the selected materials in this study will be discussed in this section. This section includes glass fiber surface cleaning and PDMS preparation which well be described in the following.

Glass Fiber Surface Cleaning

As discussed earlier, all glass fibers used in this study were produced using the same fabrication process. For the normal use, the glass fibers were dipped into acetone for about 5

minutes followed by air drying before depositing a droplet. Other surface treatment conditions will be discussed later in the appropriate chapter.

PDMS Preparation

In order to perform the micro-droplet experiments, it was necessary to prepare the PDMS for depositing on the glass fiber. The two-part components of PDMS mixture were prepared by mixing the Sylgard 184 silicone elastomeric base and the curing agent at desired ratios by weight. These two parts can be mixed in different ratio (2.5 to 50 parts per hundred (pph)) [4]. The elastic modulus of the droplet increases by increasing the mixing ratio.

Each weight ratio was measured using a high resolution balance (Explore Pro analytical balance from OHAUS). A clean plastic cup was placed on the balance, and then the balance initialized to zero reading. Some amount of silicone based Sylgard 184 was added in the cup. The weight was measure by the balance, and a desired ratio of curing agent was added to the base. The mixture was prepared by stirring with a glass rod for a few minutes at room temperature. Stirring produces air bubbles in the mixture which decreases the quality of the cured PDMS droplet. In order to minimize or eliminate the bubbles introduced in the mixing procedure, the mixture was allowed to rest in the air for 30 minutes as instructed in the Dow Corning data sheet [26].

Specimen Preparation

Small drops of the degassed mixture which were prepared previously, picked up by a fine wire, were deposited onto a glass fiber which was previously prepared for use. Up to two droplets were applied to a given fiber. These fiber/PDMS specimens, after depositing the degassed mixture of PDMS onto a fiber, were then cured in an oven at a specified temperature

and followed by self curing at room temperature for 1-4 hours prior to running the test. Although published reference has used a variety of curing temperature/time processes [4], the curing process for the fiber/droplet specimens used as the baseline in this study was 100 C for 45 minutes according to the Dow Corning data sheet for Sylgard 184. Different curing temperature and curing time are also used in this study to observe the influenced interfacial properties and will be discussed in more detail in a later section.

The dimensions of the cured specimens were measured by a digital microscope, as was described earlier, prior to testing the specimen. The embedded length of the droplets ranged from 0.6-1.0 mm, but most of the droplets had an average embedded length of 0.8 mm. The droplets most likely formed elliptical shapes, especially, in the baseline condition. A typical glass-PDMS droplet with elliptical shape can be seen in Figure 4.1.

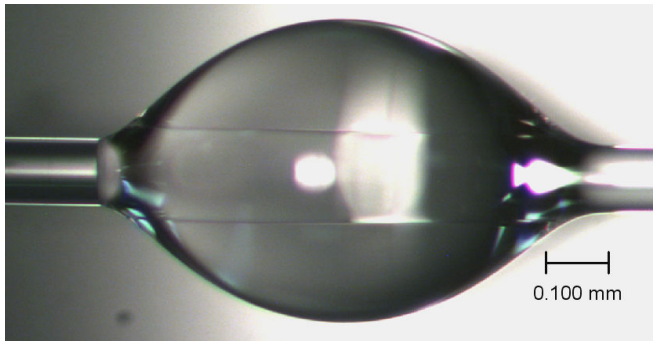

Figure 4.1 A typical smooth glass fiber-PDMS droplet with elliptical shape.

Test Evaluation

As mentioned earlier, three separate sub-studies were performed by systematically modifying the processing parameters (1) crosslinking ratio, (2) curing condition, and (3) fiber surface treatment to determine their effect on fiber/matrix adhesion of the selected material

system. Basic material/specimen preparation processes were discussed in previous sections. This section will introduce the specific modifications to these processes used in each of the three sub-studies.

- **Effect of crosslinker ratio (CHAPTER 5)** Five different PDMS-to-crosslinker weight ratios (5, 10, 20, 35, and 50 pph) were used in this study to show the influence of crosslinker ratio variation on the τ_{IFSS} – the 10 pph ratio was used as a baseline to other compositions.
- **Effect of curing conditions (CHAPTER 6)** In order to observe the influence of curing conditions, different curing temperature and curing time in addition to the baseline curing were used to change the interfacial properties.
- **Effect of fiber surface treatment (CHAPTER 7)** In order to observe the influence of the surface treatment, a fiber surface fluorination was used for surface treatment to create lower interface properties and to introduce a low adhesion between fiber/matrix surfaces.

These three parameters are thought to provide a strong case study individually. Each of them will be described in a separate chapter. Each of the chapters includes a general description and introduction of the individual case study, test evaluation matrix, the specific technique used to prepare the specimen, and results of the parameter with discussion. The next chapter will describe and evaluate the effects of the first parameter, which is effect of crosslinker ratio.

CHAPTER 5 - Effect of Crosslinker Ratio

In this chapter, the effects of crosslinker ratio on the glass fiber/PDMS droplet interfacial properties are studied. However, there is no research that has studied the interfacial properties of fiber/PDMS system using micromechanical methods. The only research [4], which is published by Deuschle et al, has studied effects of PDMS crosslinker ratios using nano-indentation test method to evaluate modulus of PDMS. It shows that an increase in the crosslinker ratio increases the modulus of the polymer. Furthermore, studies [27, 28], using glass fiber/epoxy and hemp fiber/ epoxy systems, have shown an increase of τ_{IFSS} by increasing crosslinker ratio to a limiting value beyond which τ_{IFSS} decreases. In addition, Biro et al [3], using carbon fiber/epoxy system, have shown that an increase in the fortifier ratio, which also acts as a crosslinker, also increases the τ_{IFSS}. From the reviewed literature, it shows that there is a direct relation between the modulus of elasticity and τ_{IFSS} in these fiber/matrix material systems. Therefore, an increase in the elastic modulus proportionally increases τ_{IFSS} to a limiting ratio of crosslinker where the τ_{IFSS} is highest.

From the reviewed study results, it is considered that changing crosslinker ratio of PDMS should change interfacial properties of glass fiber/ PDMS droplet system. Therefore, a range of crosslinker ratios were selected in this study to observe the effect on the interfacial shear strength of this system and compare with the reviewed studies. To describe the selected crosslinker ratios, a test matrix, which shows all of the crosslinker variations, is presented in the following section.

Test Matrix

Five different PDMS-to-crosslinker weight ratios (5, 10, 20, 35, and 50 pph) were used in this study to show the influence of crosslinker ratio variation on the τ_{IFSS}. The Dow Corning recommended PDMS mixing ratio is 10 pph of crosslinker, so the 10 pph mixture of PDMS was used as a baseline for all parts of this study. The 35 pph ratio was chosen because in [29] this ratio was shown to be the limiting value. The 50 pph was chosen to determine if the IFSS does, in fact, decrease after the expected limiting value. Table 5.1 shows a test matrix for the crosslinker ratio variations including the number of specimens that were tested for each crosslinker ratio

Table 5.1 Test matrix for the crosslinker ratios with the number of specimens tested for each ratio.

Base/curing agent ratio (pph)	# of specimens
50	6
35	10
20	6
10[a]	6
5	8

a - baseline crosslinker ratio

All of the specimens with different crosslinker ratios were cured at the baseline curing condition. As has been previously mentioned, the baseline curing condition was 45 minutes curing time at 100 C oven temperature. All of the specimens were tested at a time range

of 1-4 hours after curing. As shown in the table, 6-10 specimens were tested for each crosslinker ratio. The difference in the number of tested specimens are due to the limitation in the testing period after curing, so it was not allowed to test the specimen beyond 4 hours after curing. Therefore, a maximum number of 6-10 specimens were tested within this limited time.

Specimen Preparation and Testing

The PDMS preparation process followed the same procedure which was illustrated in the previous chapter, by mixing the two-part components of PDMS mixture with the necessary crosslinker ratio. The selected glass fiber was washed with acetone following the same procedure for the baseline surface cleaning to remove the contaminants from the surface of the fiber. The specimens were prepared by depositing a small drop of the degassed mixture onto a cleaned glass fiber surface following the method that was described previously. The geometry of the droplets formed typical elliptical shapes. A typical glass fiber/PDMS droplet was shown in Chapter 4.

All of the prepared specimens for each crosslinker ratio were tested following the test procedure introduced previously in Chapter 3, using our developed micro-droplet test setup, with two knife edges at a crosshead speed of 0.002 mm/second. The results of this test parameter will be discussed in the following section.

Results and Discussion

The interfacial shear strength (τ_{IFSS}), for all of the tested specimens with different crosslinker ratios, was calculated by equation (2.1). Table 5.2 provides an average, minimum, and maximum τ_{IFSS} and standard deviation for the different crosslinker ratios evaluated. The average values

were obtained from 6-10 specimens for each crosslinker ratio and were tested in a time range of 1-4 hours after curing the specimens.

Table 5.2 Comparative results showing maximum, minimum, and average interfacial shear strength and standard deviation

Base/curing agent ratio (pph)	# of tested specimens	τ_{IFSS} max (MPa)	τ_{IFSS} avg (MPa)	τ_{IFSS} min (MPa)	Standard deviation (MPa)
50	6	0.73	0.57	0.39	0.13
35	10	0.85	0.58	0.35	0.18
20	6	0.67	0.53	0.44	0.09
10	6	0.37	0.31	0.27	0.04
5	8	0.26	0.16	0.10	0.05

It is considered that the stress is uniformly distributed along the embedded length [8, 15], but that there is a stress concentration (meniscus) at the ends of the fiber embedded length [1] which makes determination of the actual embedded length (and therefore strength) difficult. Therefore, there is a larger scatter in the τ_{IFSS} values. The variations in the interfacial shear strength are also due to the change in embedded area of the droplet, which has been shown to cause the τ_{IFSS} to decrease as the embedded area increases [8, 15]. The results from this study also show that the embedded area has a significant influence on the variation of the τ_{IFSS} values. These variations are shown in a later figure. Furthermore, the stress concentration at the ends of the droplet [1, 13] also affects the τ_{IFSS} values. It was observed in this study that when there is a bigger stress concentration at the end of the droplet, τ_{IFSS} is also increased. Figure 5.1(a) shows that there is no stress concentration at the ends of the droplet (whole droplet debonded), while

Figure 5.1 (b) shows that there is a bigger stress concentration at the ends (droplet debonded with meniscus still bonded). Therefore, this causes τ_{IFSS} to be increased.

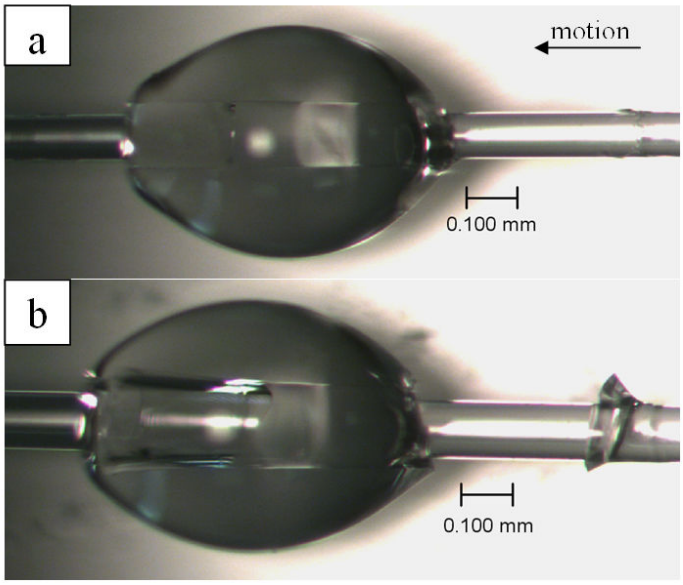

Figure 5.1 Possibilities of debonding. (a)- complete debonded (b)- meniscus left bonded

The interfacial shear strength is shown in Figure 5.2 at different crosslinking ratios. From this figure, the maximum value of τ_{IFSS} can be found at the crosslinking ratio of 35 pph by weight ratio. In this study, the τ_{IFSS} values range from 0.16 MPa for the 5 pph composition to 0.58 MPa for the 35 pph composition, which shows highest interfacial shear strength, while 0.57 MPa was obtained for 50 pph composition which decreased after 35 pph. The same trend was shown by Lili et al [27] using a glass fiber/epoxy droplet system with a greater decrease after τ_{IFSS} reaches to maximum at 34 pph. Islam et al [28] shows a similar trend using hemp fiber/ epoxy droplet in a fiber pull-out system but using different crosslinker ratios of 60 – 120 pph and obtains the highest τ_{IFSS} and tensile strength at 100 pph crosslinker ratio.

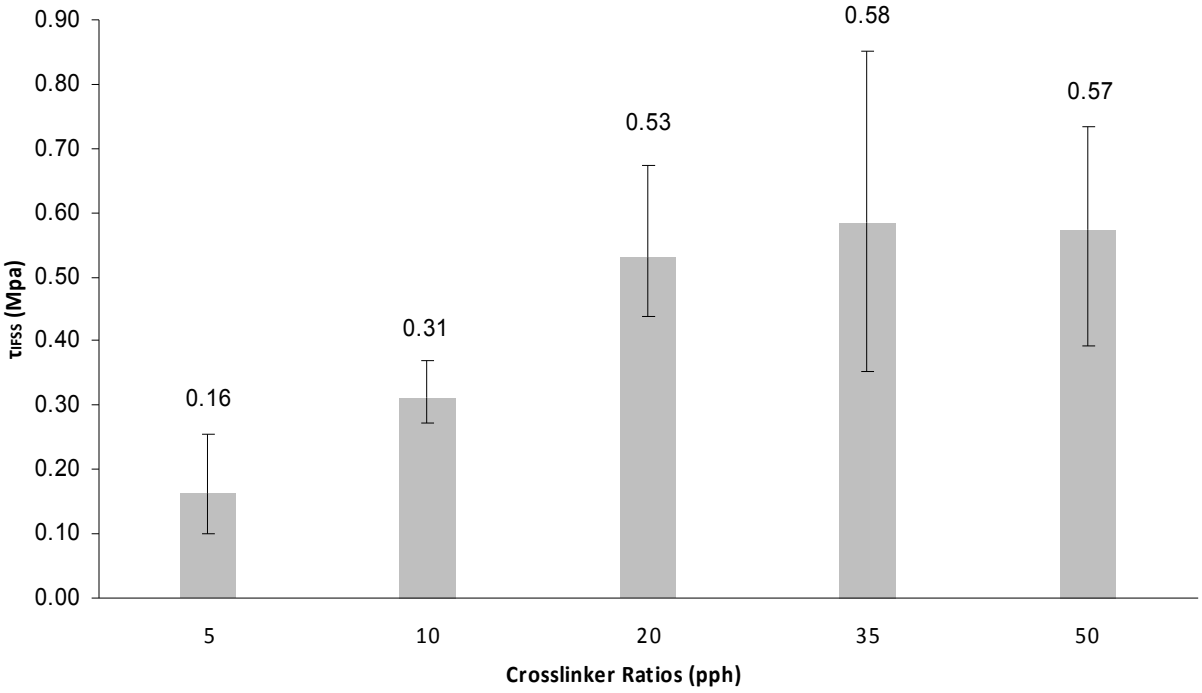

Figure 5.2 Results of all crosslinking ratios micro-droplet tests, showing their average interfacial shear strength.

The three general trends for shear force versus displacement profile were described in Figure 3.1(a, b, and c). Each of the three general trends can be seen in the results of this experiment which are shown in Figure 5.3. In this figure, the shear stress gradually increases to the debonding point. Then, the debonding occurs differently for each crosslinking ratio. The 10 pph ratio follows the trend of Figure 3.1 (b), where the stress gradually reaches the maximum and decreases gradually to a frictional shear stress. The profile for the 35 pph ratio can be interpreted as a sudden drop, as in Figure 3.1 (a), because a steeper decrease has occurred after debonding to a lower frictional force. The trend illustrated in Figure 3.1(c) can be seen for 5 pph, 20 pph, and 50 pph, where slippage occurs. The decrease from the peak has occurred as a sudden drop in the 50 pph profile with a lower frictional shear stress, while the debonding has occurred

gradually in the profiles for 5 pph and 20 pph with a higher frictional shear stress. All of these illustrated possible debonding trends have been visually observed by a microscope during the experiment. The largest drop in peak shows the strongest interface [28]. In agreement with this, the shear stress versus displacement profile of 35 pph shows the largest drop indicating the strongest interface, while the shear stress versus displacement profile of 5 pph shows the smallest drop indicating the weakest interface.

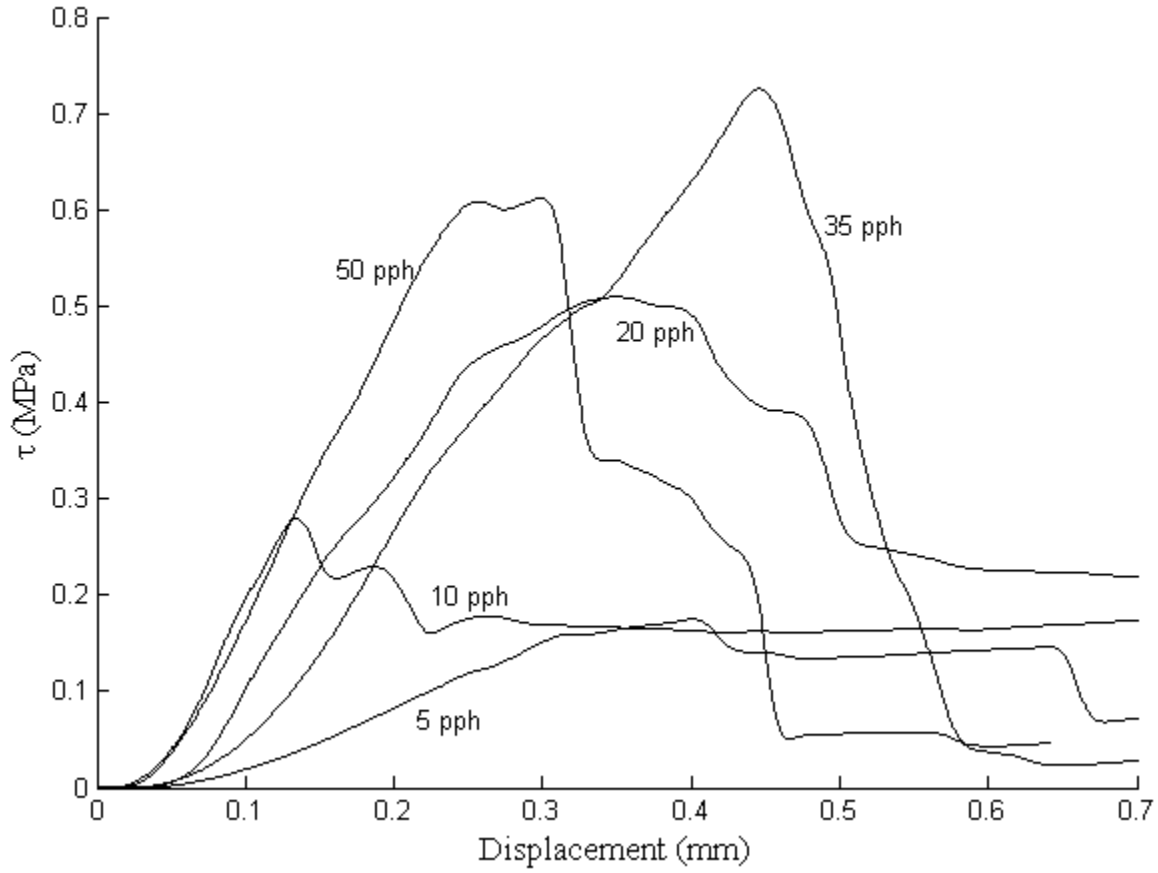

Figure 5.3 Stress versus displacement plot for different crosslinker ratios, 5 pph, 10 pph, 20 pph, 35 pph, and 50 pph, where 35 pph shows the highest adhesion.

The shear stress versus displacement profile of all the tested specimens with baseline crosslinker ratio is also shown in Figure 5.4. The scatter in this figure has occurred due the factors which were described earlier.

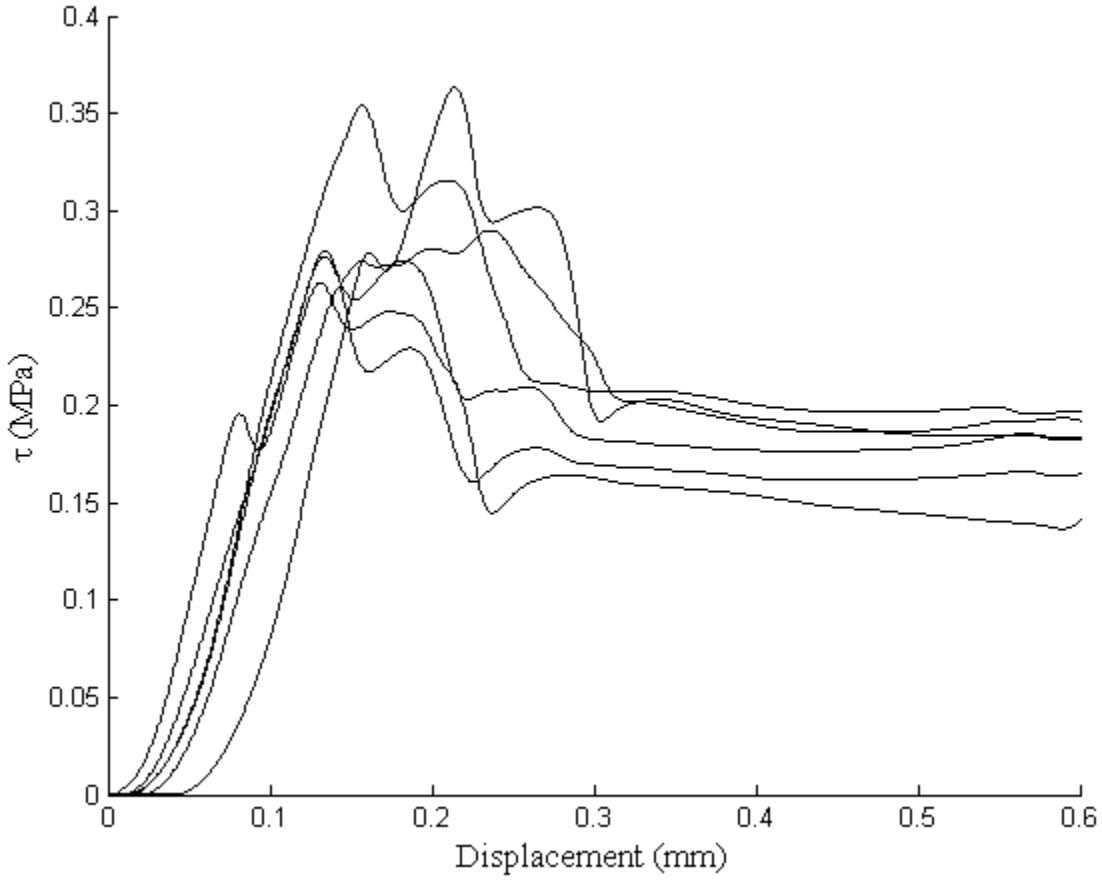

Figure 5.4 Stress versus displacement plot of all the specimens tested at baseline crosslinker ratio

Furthermore, in Figure 5.3, the slope of the largest crosslinker is steeper than the smallest crosslinker ratio. It should be noted however that the fiber diameters were not the same for all cases. An increase in slope can still be distinguished in each profile as the crosslinker ratio increases. Only the profile for the 10 pph ratio does not follow this trend because the fiber diameter of the specimen was significantly smaller than other cases. Otherwise, it would have

followed the described trend. The slope was expected to behave in this manner because well bonded chain segments due to rising crosslinker ratio influences the modulus of polymer, and the modulus is related to the slope. As the modulus increases, the material tends to behave more brittle, and the material fractures more abruptly after reaching the brittle condition. Therefore, the adhesion between fiber and matrix decreases, so the τ_{IFSS} is highest during the transition from ductile to brittle properties. The relation between modulus and τ_{IFSS} during the transition is illustrated in Figure 5.5.

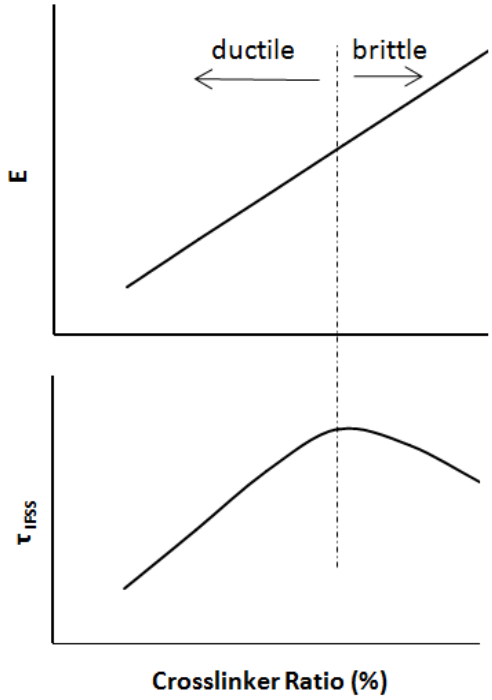

Figure 5.5 The relation between modulus and τ_{IFSS} of PDMS with change in crosslinker ratio.

This finding can be compared with results from Deuschle et al [4], which indicate that an increase in crosslinker ratio increases modulus of the polymer, while the Poison's ratio decreases due to the increment of crosslinker ratio, thus the material gets stiffer. When the material gets stiffer due to the increment of crosslinker ratio, the "dangling" chain segments between

molecules get shorter. As the chains get shorter, the material properties change to brittle. This situation is believed to have the highest interface.

The yield strength and tensile strength obtained from [27, 28], which display the same trend as τ_{IFSS}, also support the results of this study because they are related to the adhesion and indicates the same peak in strengths when the material transitions to brittle. The next chapter will describe the evaluation of the second parameter introduced in Chapter 4, which is the effect of curing condition including different curing time and temperature.

CHAPTER 6 - Effect of Curing Conditions

In this chapter, the effects of different curing conditions on the glass fiber/PDMS droplet interfacial shear strength are studied. It is already mentioned in previous chapter that there has not been any micromechanical research conducted to study the interfacial properties of glass fiber/PDMS system. Previous research [4], using the nano-indentation method, shows that curing time or temperature can influence the elastic modulus of the polymer network which is a direct indication of polymer network variation. The increase in curing time and temperature was also shown by [3, 29], using carbon fiber /epoxy and monofilament glass fiber/vinylester systems, which shows an increase in τ_{IFSS} to a limiting value before decreasing. This shows the direct relation of elastic modulus and τ_{IFSS} properties.

Based on the results of the presented research, it is considered that changing PDMS curing time or temperature may influence interfacial properties of the glass fiber/ PDMS droplet system. Therefore, various curing times and temperatures (including the Dow Corning curing recommendation for the baseline case) were logically selected in this study to evaluate possible changes that may be caused by curing condition. A test evaluation matrix will be presented in the following section to describe the selected curing times and temperature for this study.

Test Matrix

A series of numbers and letters are used to designate the curing conditions used in this study. The number of hours the specimen was cured is the first number in the designation, followed by an "H" to denote hours. The temperature (in degrees Celsius) follows the "H", followed by a "C" to denote degrees Celsius. If curing was performed at room temperature, "RT" follows the "H" rather than a temperature.

Four different glass fiber/PDMS micro-droplet specimen curing conditions (2H75C, 2H100C, 4H100C, 48HRT), in addition to the baseline curing, were used in this study to show the influence of curing condition on the τ_{IFSS} values. These curing conditions will be compared with the baseline curing condition which is 45 minutes curing at 100 C. The 48HRT condition was an alternative recommendation to the baseline curing from Dow Corning. Table 6.1 shows the test matrix of the curing types including curing time, curing temperature, and number of specimens that were tested for each curing type. All of the specimens were tested at the same time range of 1-4 hours after curing, as was mentioned in previous chapter, and the difference in the number of tested specimens are also due to the limitation in the testing period after curing.

Table 6.1 Curing conditions for glass fiber/PDMS

Type	Curing schedule	No. of specimens
Baseline	45 min cure @100C	6
2H75C	2 h cure @ 75 C	6
2H100C	2 h cure @ 100 C	8
4H100C	4 h cure @ 100 C	10
48HRT	48 h cure @ RT	9

Specimen Preparation and Testing

The PDMS preparation process followed the same procedure which was illustrated in Chapter 4, by mixing the two-part components of PDMS mixture with a crosslinking ratio of 10 pph for all specimens in the matrix. Each glass fiber was washed with acetone following the same procedure as baseline cleaning. The specimens for all of the curing types were prepared by

depositing two small droplets of degassed PDMS mixture onto a glass fiber following the baseline procedure. The curing procedure was conducted for each type following the curing schedule in Table 6.1 after depositing of droplets. The geometry of the droplets formed elliptical shapes, similar to previous specimens.

The testing procedure for each of the curing conditions followed the same method which was introduced in Chapter 3, using two knife edges with a crosshead speed of 0.002 mm/second. The specimens were tested at a time range of 1-4 hours and were kept in a desiccator following the end of the specified cure cycle.

Results and Discussion

The interfacial shear strength (τ_{IFSS}), for all of the tested specimens with different curing conditions, was calculated by equation (2.1). Table 6.2 provides an average, minimum, maximum, and standard deviation for the τ_{IFSS} results of different curing conditions. These values were obtained from 6-10 specimens for each curing type.

Table 6.2 Comparative results showing maximum, minimum, average, and standard deviation for interfacial shear strength results of different curing conditions

Curing condition	No. of tested specimens	τ_{IFSS} max (MPa)	τ_{IFSS} avg (MPa)	τ_{IFSS} min (MPa)	Standard deviation (MPa)
Baseline	6	0.37	0.31	0.27	0.04
2H75C	6	0.57	0.39	0.29	0.11
2H100C	8	0.91	0.71	0.55	0.12
4H100C	10	0.90	0.72	0.47	0.14
48HRT	9	0.38	0.25	0.15	0.08

The distribution of the stress along the embedded area was considered the same as the previous chapter, and the stress concentration (meniscus) at the ends of the fiber embedded length and the changes in embedded area were the major factors that caused the variation of the τ_{IFSS}, as have been described in detail previously in Chapter 5.

The interfacial shear strength (τ_{IFSS}) is shown in Figure 6.1 at the different curing conditions tested. From this figure, a representative maximum value for τ_{IFSS} can be found at 4H100C, which is 4 hours curing at 100 C. In this study, the average τ_{IFSS} values range from 0.25 MPa for the 48HRT condition to 0.72 MPa for the 4H100C condition, which exhibits the highest interfacial shear strength. The results shown by [3, 29], using carbon fiber/epoxy droplet and monofilament glass fiber/vinylester droplet in micro-droplet system with different curing schedule, indicate that a higher curing temperature for longer time has introduced a stronger interfacial shear strength when the specimen is fully cured. However, after a limiting time in [29], τ_{IFSS} has decreased. In our study, the curing was not performed over a long period of time. The τ_{IFSS} has increased from baseline to 2H100C curing condition, which are cured under the same temperature, and reached a plateau at 4H100C with a little further increase. This indicates that the specimen was almost fully cured after two hours since crosslinking reaction slows down during the curing process and that four hour curing may cause an increase in the modulus of elasticity of the PDMS with a slight change in the τ_{IFSS} value. Longer curing time of up to ten hours [4] is needed for the PDMS to be fully cured to obtain higher modulus and can improve the interface interaction of fiber/matrix system and enhances the stress transfer from matrix to fiber [29]. In addition, these two curing conditions gave results two-fold higher than that of 2H75C. It has been shown by Biro et al [3] that the higher curing temperature has a significant influence on

increasing the interfacial shear strength because it increases the motion of segmental chains. Especially when the curing temperature is above the glass transition temperature (T_g) of the polymer, the interfacial shear strength reaches its maximum strength. However, in our case, the variation of curing temperature was not in the range of T_g. The glass transition temperature for PDMS is above 150 C. The τ_{IFSS} obtained from baseline curing condition is higher than 48HRT curing condition. However, both were Dow Corning curing recommendation. Since higher temperature forms more crosslinking points, it accelerates the curing process. On the other hand, since the diffusion velocity [4] at lower temperature is reduced, the duration of the crosslinking reaction will be prolonged. Thus, the mechanical properties at lower curing temperature do not reach the same level as for higher curing temperature even if it is cured for a longer time.

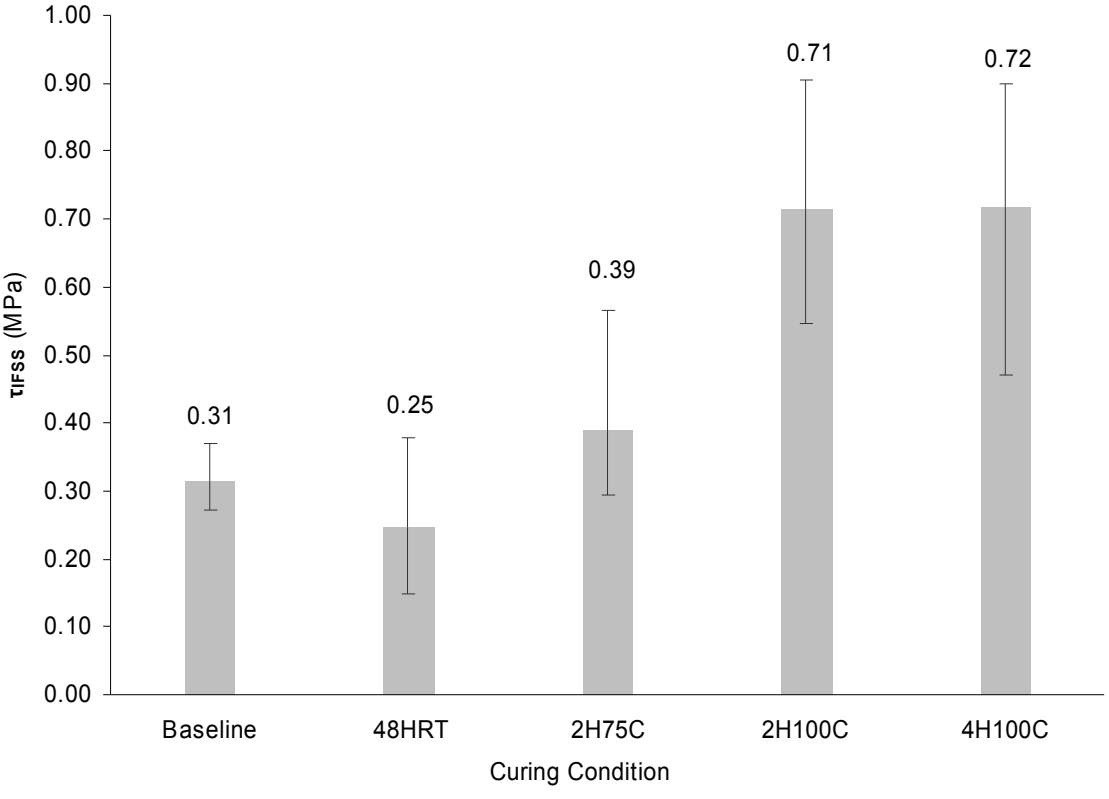

Figure 6.1 Results of all curing conditions showing their average interfacial shear strength.

The three general trends for shear stress versus displacement profile, which were described in Chapter 3, can also be observed in the results of the curing conditions in Figure 6.2. The largest drop in this figure occurs in 4H100C which has the strongest interfacial shear strength, while 48HRT curing condition exhibits the smallest drop indicating the weakest interface.

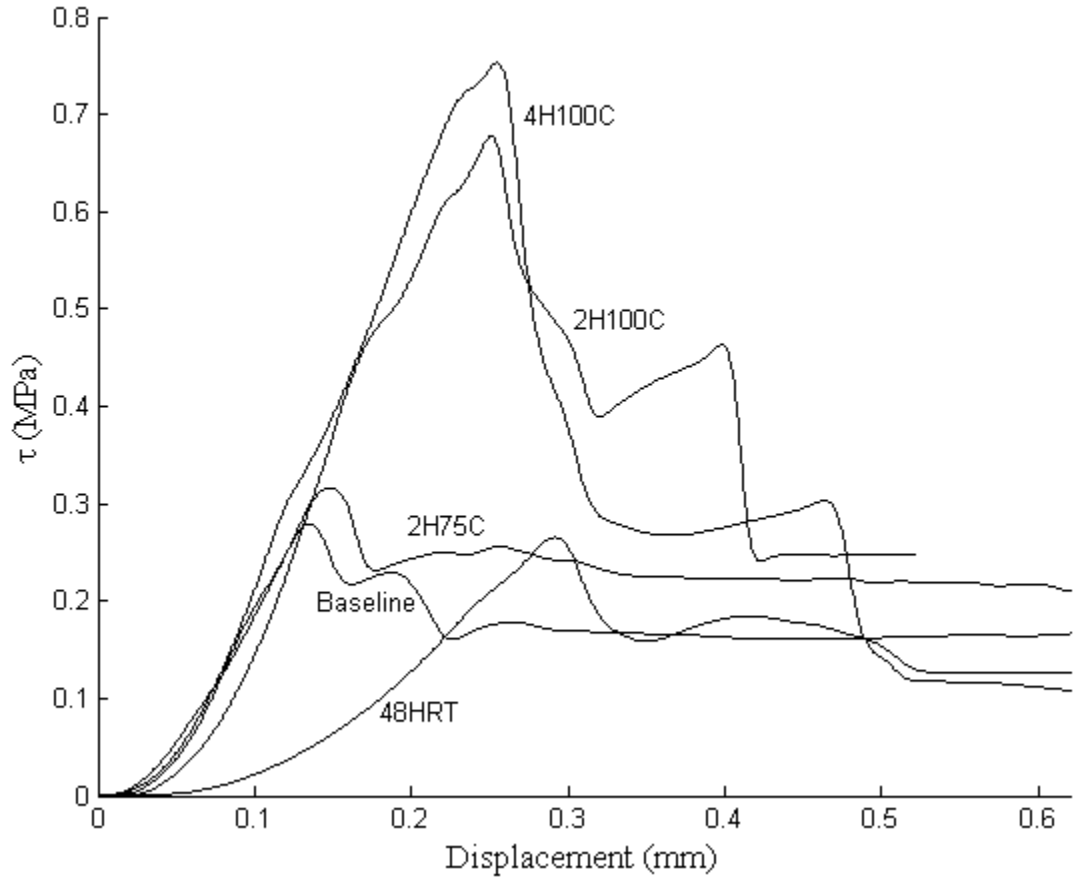

Figure 6.2 Typical stress versus displacement plot for different curing conditions (Baseline, 48HRT, 2H75C, 2H100C, and 4H100C.)

The shear stress versus displacement profile of all the specimens tested in 4H100C curing condition is also shown in Figure 6.3 to compare the trends at same curing condition. The scatter is caused due to embedded area and meniscus as mentioned in previous chapter.

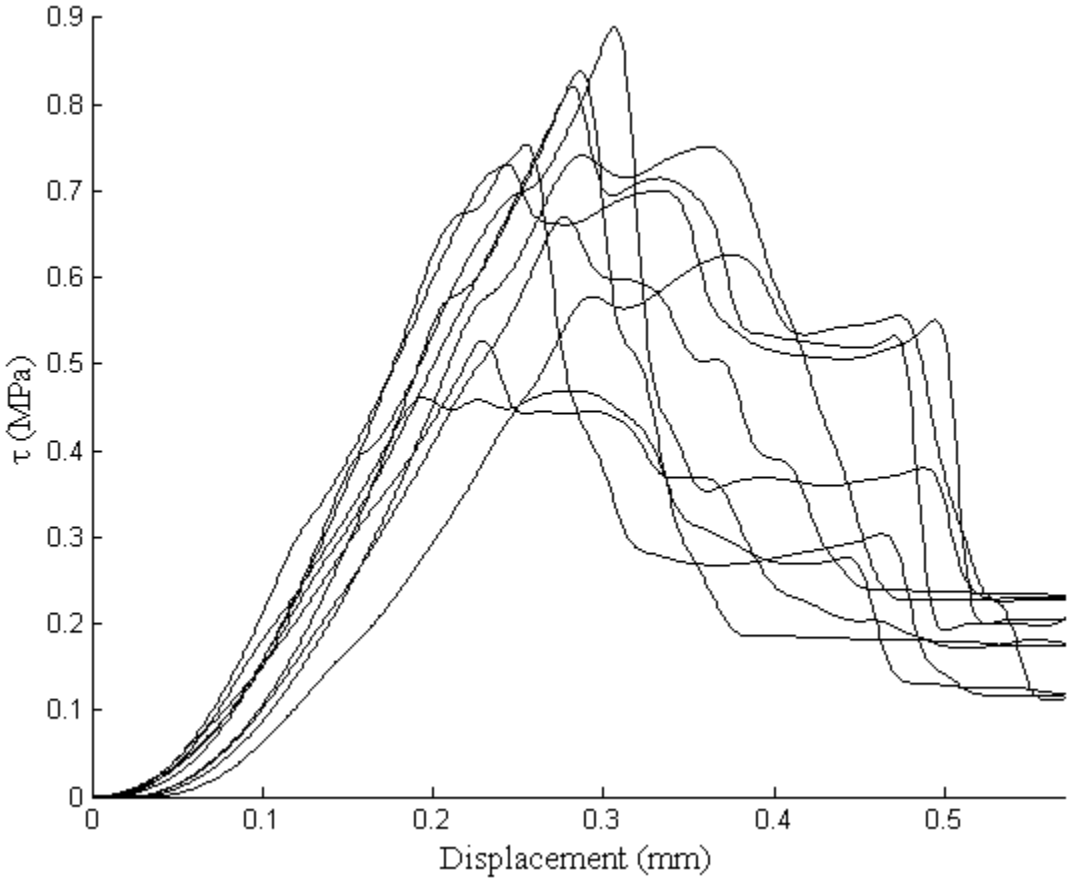

Figure 6.3 Stress versus displacement plot of all the specimens tested at 4H100C curing condition

Furthermore, the slope of the higher temperature and longer curing time is steeper than the lower temperature and shorter curing time. The higher temperature and longer curing time result in better adhesion and well bonded chain segments because higher curing temperature

accelerates the bonding process due to creation of more crosslinking points, and additional chemical reaction can be possible [4].

The shear stress versus displacement profiles of the baseline and 48HRT conditions, which both were Dow Corning curing recommendation, show that there is a big difference in the slope. The slope of baseline is significantly larger than that of 48HRT. However, the fiber diameter of 48HRT was a little larger than other curing conditions. This slope indicates that higher temperature over a short period of time has accelerated the curing process and increased the modulus, whose relation was described earlier in Chapter 5, and the reduction in the diffusion velocity in low temperature caused a deceleration in the curing process and a decrease in the slope which relates to modulus. However, according to the Dow Corning curing schedule, both curing conditions have almost the same interfacial shear strength with a slight increase in the baseline curing schedule response because higher curing temperature rapidly improves the interfacial properties and curing process, while lower temperature slows down the curing process. The next chapter will describe the evaluation of the third parameter introduced in Chapter 4, which is evaluation of the effects of surface treatment on τ_{IFSS} properties.

CHAPTER 7 - Effect of Surface Treatment

As mentioned earlier, the goal of this work is to understand the relationship between mechanical performance of a model glass fiber/polymer system and the chemical interactions that occur at the glass fiber/polymer interface. In previous chapters, the effects of different polymer structures on the adhesion behavior of glass fiber/ PDMS droplets were investigated. This chapter discusses the effect of glass fiber surface treatment on the interfacial shear strength of glass fiber/ PDMS system. Surface treatment has been shown to be an effective way to alter the interfacial shear strength between two materials through modifying the surface chemistry of one or both materials without changing their bulk properties. Surface modification of one surface affects the ability of that surface to interact and develop bonds with the opposite surface.

For the purposes of this study, the surface fluorination, which is expected to decrease the interfacial shear strength, is used. This functionalization was chosen over ones that would increase τ_{IFSS}. The following sections will introduce the surface treatment process and the results of interfacial behavior of glass fiber/PDMS as a function of surface modification. These results can provide an understanding of the correlation between mechanical performances of a system at the macroscopic level and to the bonds formed at the interface of two surfaces at the molecular level.

Surface Treatment

One of the most convenient ways to modify the surface structure of a material is to introduce functional groups at the surface of that material by means of a coupling agent. Typically, silane based agents are used for treating glass surfaces. Silanes are silicone based chemicals with two active ends, R and X, illustrated in Figure 7.1 (a). In the silane structure, one

end (X in Figure 7.1) can react with glass substrates and leaves behind a specific functional group (R) on the glass surface (see Figure 7.1 (b)). The functional group introduced at the glass surface can alter the interaction of the glass surface with the other surface (or the polymer in our case).

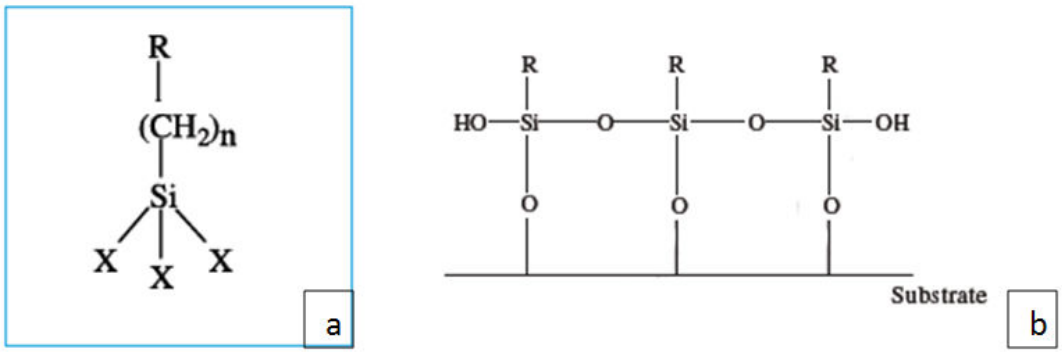

Figure 7.1 The general formula of a silane agent (a), and the configuration of the treated surface (b) [30]

In this study, a silane based agent was desired for surface modification of glass fiber to decrease the interfacial shear strength of glass fiber/ PDMS micro-droplet system. Therefore, 1H,1H,2H,2H-Perfluorodecyltrichlorosilane (FDTS, $CF_3(CF_2)_7(CH_2)_2SiCl_3$ from Alfa Aesar) was selected for use as the silane based coupling agent for the glass fiber surface treatment. Since FDTS cannot be used without a solvent to make a solution, hexane (from Fisher Scientific) was selected as solvent of FDTS. As noted, FDTS is expected to decrease τ_{IFSS} because of its non-polarity (i.e. the electrons are equally shared between different atoms and there is no hydrogen bonding) which results to a low surface energy, as shown in Figure 7.2. Decrease in τ_{IFSS} should also accompanied increase of glass fiber/PDMS droplet contact angle. In addition, increase in contact angle also has an inverse relation to decrease the surface energy, surface tension, and surface wettability, which all can be calculated from contact angle measurement. It

should be noted, that in this context the glass fiber/PDMS droplet contact angle is referring to the angle of the PDMS droplet with the surface of glass fiber as was used elsewhere by Sun et al [27] and Wu et al [31].

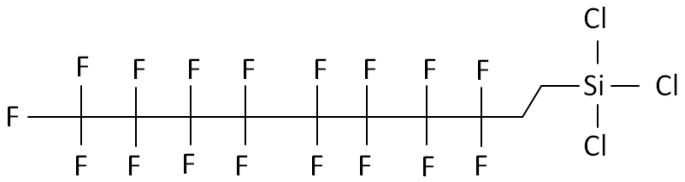

Figure 7.2 Molecular structure of FDTS

It was shown by Choi et al [32] that FDTS coating agent (using three different film thickness) for the amorphous carbon surfaces has significantly increased the contact angle (using water as the probe liquid) and also decreased the spreading distance (wetting) of perfluoropolyethers (PFPE) as FDTS average coated film thickness increased. Clark et al [33], using three different fluoride salts as surface treatments to the surface of E-glass, have shown that the surface tension significantly decreased as the glass fiber contact angle (using water as the liquid) increased due to extent fluorination of the surface.

Test Matrix

In this section of our study, the baseline form of PDMS mixture (10 pph crosslinker ratio) was used to make micro-droplet specimens. Table 7.1 shows a test matrix for both acetone cleaned surface and FDTS treated surface including the number of specimens that were tested for each crosslinker ratio

Table 7.1 Test matrix for the non-treated and treated surfaces with the number of specimens tested for each condition.

Type of surface	# of specimens
Baseline	6
FDTS	6

All of the FDTS treated specimens were cured the same as the baseline curing condition. As has been previously mentioned, the baseline curing condition was 45 minutes curing time at 100 C oven temperature. All of the specimens were tested at the same time range of 1-4 hours after curing, as was mentioned in previous chapters.

Specimen Preparation and Testing

The PDMS preparation process followed the same procedure which was illustrated in Chapter 4, by mixing the two-part components of PDMS mixture with a crosslinking ratio of 10 pph for all specimens in the matrix. All glass fibers were acetone washed. In order to prepare the fluorinated fibers, acetone washed fibers were dipped into a small amount of FDTS dissolved in Hexane with 0.5% weight ratio for about five minutes and followed by air drying. Then, the degassed PDMS was deposited on to the surface of the fiber to make two droplets.

All of the prepared specimens for the baseline and fluorinated surface were tested following the test procedure introduced previously in Chapter 3, using our developed micro-droplet test setup, with two knife edges at a crosshead speed of 0.002 mm/second. The results of this test parameter will be discussed in the following section.

Results and Discussion

The interfacial shear strength (τ_{IFSS}), for all of the tested specimens, was calculated by equation (2.1). Table 7.2 provides an average, minimum, maximum, and standard deviation for the τ_{IFSS} results and also gives the average glass fiber/ PDMS contact angle of the baseline and FDTS treated specimens. These values were obtained from 6 specimens for each type.

Table 7.2 Comparative results showing maximum, minimum, average, and standard deviation interfacial shear strength results with average contact angle

Surface type	# of tested specimens	τ_{IFSS} max (MPa)	τ_{IFSS} avg (MPa)	τ_{IFSS} min (MPa)	Standard deviation (MPa)	Contact angle (deg)
Baseline	6	0.37	0.31	0.27	0.04	34.75
FDTS	6	0.20	0.16	0.12	0.03	49.24

The distribution of the stress along the embedded area was considered the same as the previous chapter, and the stress concentration (meniscus) at the ends of the fiber embedded length and the changes in embedded area were the major factors that caused the variation of the τ_{IFSS} , as have been described in detail previously in Chapter 5.

The interfacial shear strength, for baseline and FDTS treated surface, is shown in Figure 7.3. From this figure the value of τ_{IFSS} for baseline (0.31 MPa) is two folds higher than that of FDTS treated surface (0.16 MPa), because FDTS surface treatment has decreased the surface tension and surface energy of the glass fiber which was obtained by Choi et al [32] and Clark et al [33] using FDTS-coated amorphous carbon surfaces and fluoride salts on E-glass surface.

Therefore, low surface energy of a fluorinated surface causes low interfacial shear strength, as was described earlier.

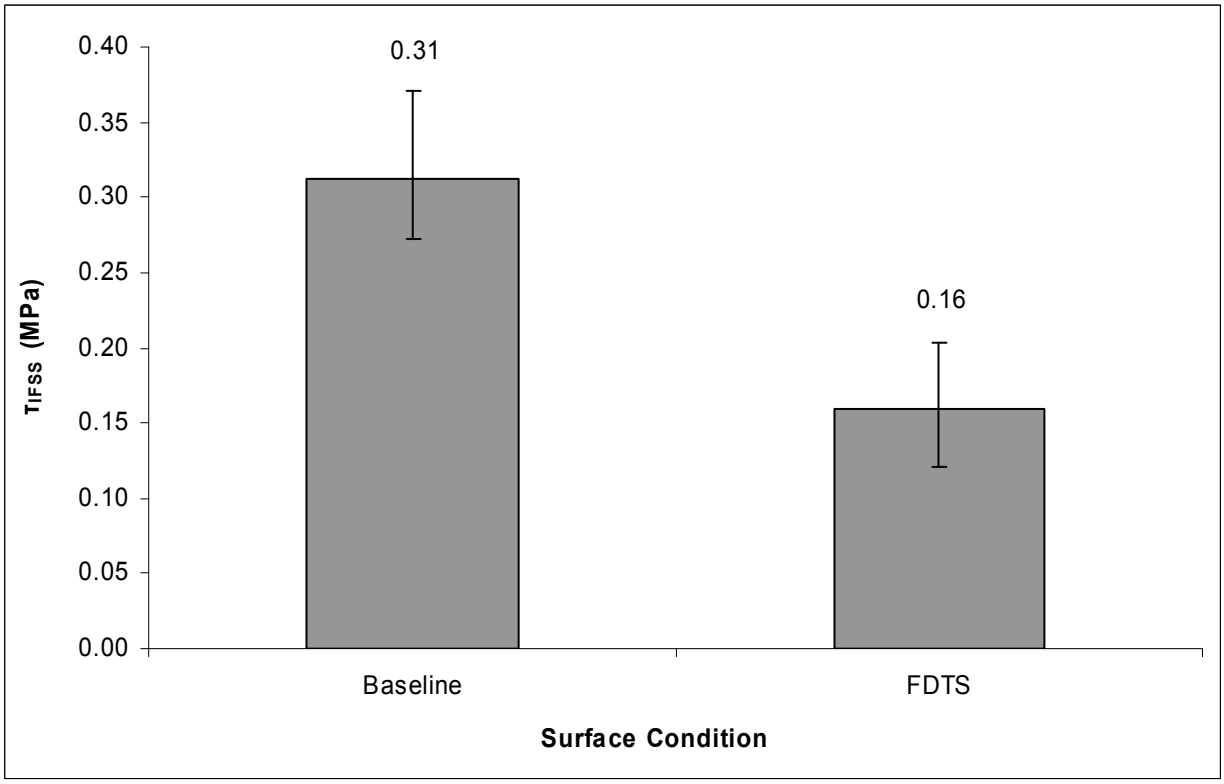

Figure 7.3 Results of baseline and FDTS surface treated micro-droplet tests, showing the average interfacial shear strength.

Figure 7.4 (a and b) show typical micro-droplet specimens with measured contact angle. In Figure 7.4 (b), the geometry of the droplets on the fluorinated surface has formed more spherical shape rather than elliptical which can be seen in baseline case, Figure 7.4 (a). Therefore the glass fiber /PDMS droplet contact angle is increased when the glass fiber surface was treated by FDTS. Figure 7.5 shows average glass fiber/ PDMS droplet contact angles measured from both baseline and FDTS treated micro-droplet specimens with error bars, where the contact angle is significantly increased for FDTS treated case. This is due to the formation of Si-F group on the

surface of the glass fiber to increase glass fiber/ PDMS droplet contact angle [33]. When the surface does not have good wettability, there is not a good stress transfer, so the τ_{IFSS} decreases.

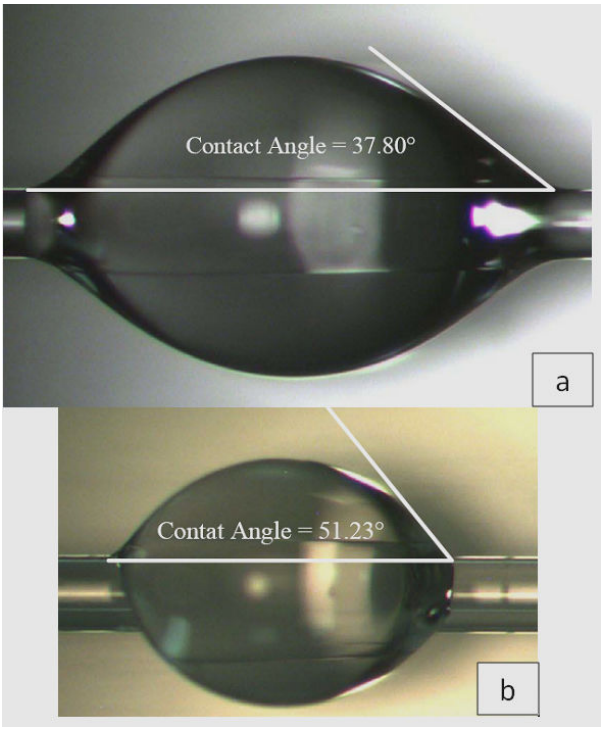

Figure 7.4 Contact angle measurement- (a) baseline and (b) FDTS treated

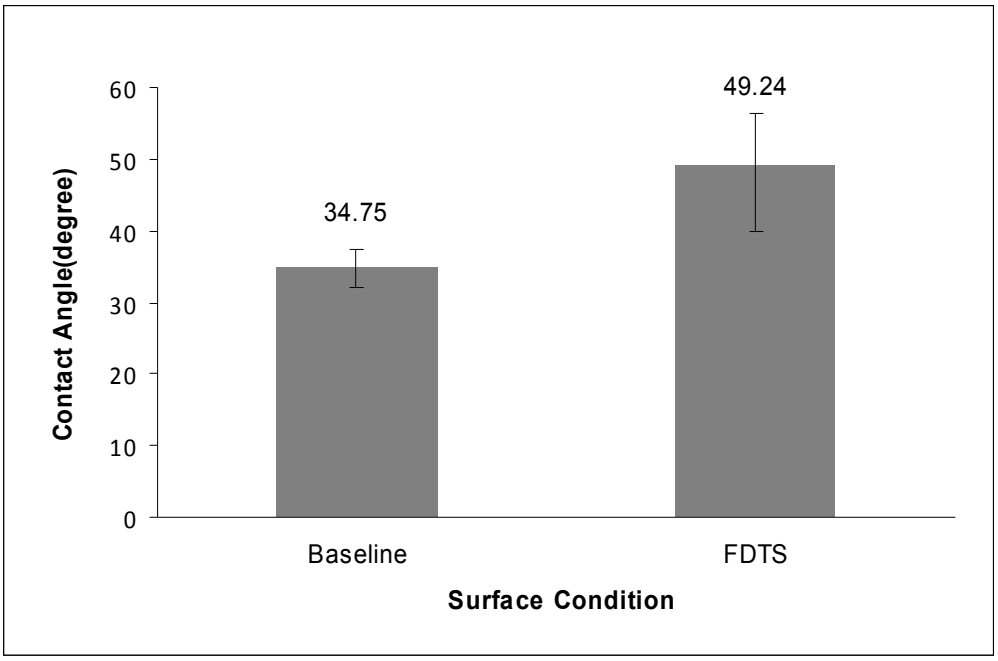

Figure 7.5 Results of baseline and FDTS surface treated micro-droplet tests, showing their average contact angle

The three general trends for shear stress versus displacement profile were described in Figure 3.1(a, b, and c). Both of the baseline and FDTS follow the trend of Figure 3.1 (b), where the stress gradually reaches the maximum and decreases gradually to a frictional shear stress as shown in Figure 7.6. The largest (relative) drop in peak shows the strongest interface [28]. In agreement with this, the shear stress versus displacement profile of the baseline case shows the larger (relative) drop indicating the stronger interface, while the shear stress versus displacement profile of FDTS shows a very small drop, and the frictional stress of FDTS is almost equal to the peak, which shows a very weak interface bonding.

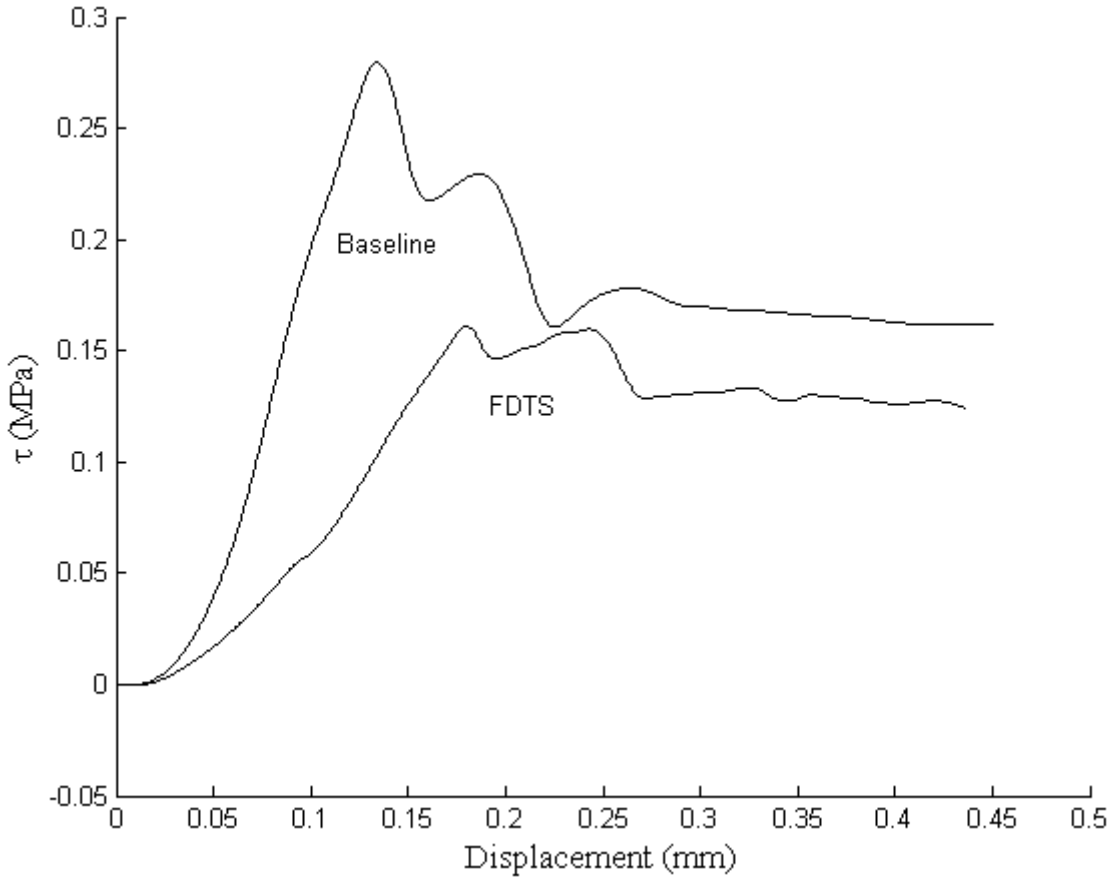

Figure 7.6 Typical stress versus displacement plots for baseline and FDTS treated droplets.

The shear stress versus displacement profile of all the FDTS tested specimens is also shown in Figure 7.7 to compare the trends. The scatter is due to the factors which were described in previous chapters.

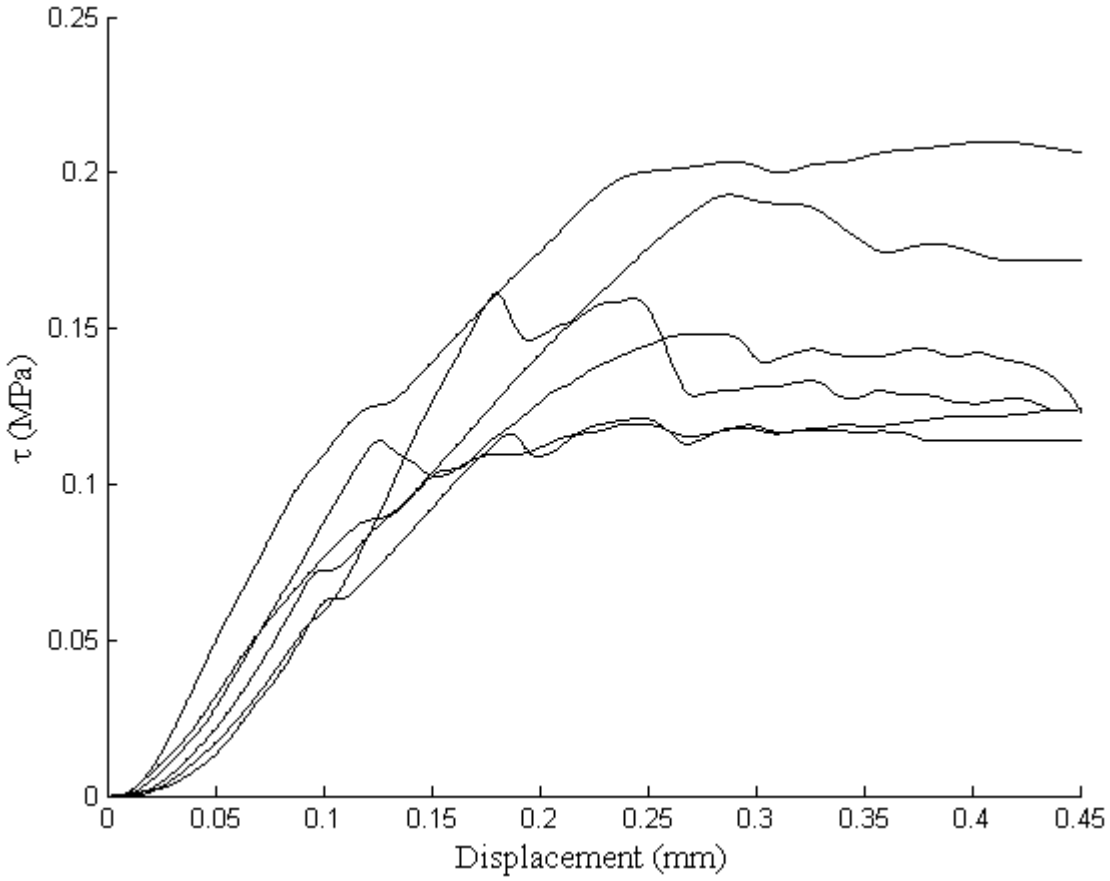

Figure 7.7 Stress versus displacement plot of all the tested FDTS treated specimens

Furthermore, in Figure 7.6, the slope of baseline is steeper than the slope of FDTS treated glass fiber surface. It should be noted however that the fiber diameters of FDTS treated specimens were larger than baseline specimens. The slope also shows that FDTS treated surface has decreased the surface wettability, and the bond strength is reduced. The results show the important roles of both surface structure and interfacial properties in the well bonding (performance) and interfacial shear strength of the system. Therefore, surface treatment is crucial in the interfacial performance of the system. The next chapter will provide overall conclusions for this study.

CHAPTER 8 - Conclusions and Recommendations

As stated in Chapter 1, four goals were accomplished in this research. The first goal was to develop and set up the experimental micro-droplet test apparatus. The second goal was to evaluate the effect of different crosslinking ratios to the variation of interfacial shear strength of a fiber/polymer micro-droplet system. The third goal was to evaluate the effects of curing conditions to the interfacial shear strength of fiber/polymer micro-droplet systems. The last goal was to see how surface modification may affect the interfacial properties of the glass fiber/polymer micro-droplet systems. Self modified borosilicate glass rod (glass fiber) and PDMS were used as reinforced fiber and matrix for all of these studies. The following conclusions were found from the results of this research.

Conclusions

The following list of conclusions is found based on the results of this research to satisfy the required goals:

1. The micro-droplet apparatus was designed, built, and used in the testing of the selected glass fiber and PDMS. This micro-droplet setup meets the requirements to be used as micromechanical testing equipment.
2. The literature and this study show that a small error is inherent in the micro-droplet test results due to not being able to control the geometry the same for all micro-droplet specimens.
3. Formation of stress concentration (meniscus) at the ends of droplet plays a significant role to affect the result of the interfacial shear strength.

4. The interfacial shear strength of glass fiber/ PDMS system increases when the crosslinker ratio increases to a limiting ratio of 35 pph. After that the interfacial shear strength decreases when the crosslinking ratio increases. This limiting point may be related to the PDMS transition from ductile to more brittle behavior.
5. Curing conditions also affects the interfacial shear strength of glass fiber/ PDMS system. Higher curing temperature increases the interfacial shear strength due to increasing motion of segmental chains. Higher curing temperature also forms more crosslinking points to accelerate curing process. On the other hand, mechanical properties at lower curing temperature do not reach the same level as for higher curing temperature even if it is cured for a longer curing time.
6. Glass fiber surface fluorination exhibited a significant effect to the interfacial shear strength of glass fiber /PDMS micro-droplet system as well as the glass fiber/PDMS droplet contact angle measurement. The interfacial shear strength of surface fluorinated glass fiber/ PDMS dropped down to half of as was tested at baseline condition, while the glass fiber/PDMS droplet contact angle increased due to surface fluorination of glass fiber /PDMS micro-droplet system.

Recommendations

Some possible future work based on the results and conclusions of this research are listed as following:

1. The micro-droplet test method can be used to study the fiber/matrix moisture effects on the interfacial shear strength.

2. A scanning electron microscopic analysis of the geometry and surface of fiber/matrix micro-droplet would give more information about how to reduce the errors in micro-droplets system to its minimum.
3. A numerical micro-droplet method can be modeled to calculated the interfacial shear strength and compare with the experimental results.
4. As was mentioned, glass fibers (glass rods) can be used as alternative reinforced fibers instead of wood fibers to apply the micro-droplet test method in wood adhesives because producing wood fibers in small sized are hard.

References

1. Gao, X., Et al. (2008), Effect of Fiber Surface Texture Created from Silane Blends on the Strength and Energy Obsorption of the Glass Fiber/Epoxy Interface. *Journal of Composite Materials;* 42: 513.
2. McDonough, W.G., Antonucci, J.M, and Dunkers, J.P. (2001), Interfacial shear strengths of dental resin-glass fibers by the microbond test. *Dental Materials;* 17: 492-498.
3. Biro, D.A., McLean, P., and Deslandes, Y. (1991), Application of the Microbond Technique: Characterization of Carbon Fiber-Epoxy Interfaces. *Polymer Engineering and Science;* 37: 1250-1256.
4. Deuschle, J.K., Et al. (2010), Nanoindentation studies on crosslinking and curing effects of PDMS. *International Journal of Materials Research;* 101: 1014-1023.
5. Li, J., Sun, F.F. (2009), The Effect of Maleic Anhydride Graft on the Interfacial Adhesion of Carbon Fiber Reinforced Thermoplastic Polystyrene Composite.
6. Gao, X. (2006), TAILORED INTEPHASE STRUCTURE FOR IMPROVED STRENGTH AND ENERGY ABSORPTION OF COMPOSITES, PhD's Dissertation. *University of Delaware.*
7. Brandford, D. H. (1997), Evaluation of Fiber-Matrix Adhesion Using the Single Fiber Fragmentation Test, MS Thesis. *Kansas State University.*
8. Miller, B., Muri, P., and Rebenfeld, L. (1987), A Microbond Method for Determination of the Shear Strength of a Fiber/Resin Interface. *Composite Science and Technology;* 28: 17-32.
9. Zhandarov, S.F., Mader, E., and Yurkevich, O.R. (2002). Indirect estimation of fiber/polymer bond strength and interfacial friction from maximum load values recorded

in the microbond and pull-out tests, Part 1: load bond strength. *J. Adhesion Sci. Technol.;* 16: 1171-1200.

10. Choi, N.S., Et al. (2009), Quasi-Disk Type Microbond Pull-Out Test for Evaluating Fiber/Matrix Adhesion in Composites. *Journal of Composite Materials*, 43: 1663.
11. Trejo-O'reilly, J. A., Et al. (2000), Interfacial Properties of Regenerated Cellulose Fiber/Polystyrene Composite Materials. Effect of the Coupling Agent's Structure on the Micromechanical Behavior. *Polymer Composites;* 21:65-71.
12. Wada, A. and Fukuda, H. (1999), Microbond and Fragmentation Tests for the Fiber/Matrix Interfacial Shear Strength. *Materials Science Research International;* 5: 151-156.
13. Kang, S.K., Lee, D.B., and Choi, N.S. (2009), Fiber epoxy interfacial shear strength measured by the microdroplet test. *Composites Science and Technology;* 69: 245-251.
14. Park, J.M., Et al. (2002), Interfacial and Microfailure Modes of Electrodeposited Carbon Fiber/Epoxy-PEI Composites by Mcirodroplet and Surface Wettability Tests. *Journal of Colloid and Interface Science;* 249: 62-77.
15. Gaur, U., Miller B. (1989), Microbond Method for Determination of the Shear Strength of a Fiber/Resin Interface: Evaluation of Experimental Parameters. *Composites Science and Technology,* 34: 35-51.
16. Czigany, T., Morlin, B., Mezey, Z. (2007), Interfacial adhesion in fully and partially biodegradable polymer composites examined with microdroplet test and acoustic emission. *Composite Interfaces,* 14: 869-878.

17. Cho, D., Et al. (2009), Cellulose-Based Natural Fiber Topography and the Interfacial Shear Strength of Henequen/Unsaturated Polyester Composites: Influence of Water and Alkali Treatments. *Composite Interface,* 16: 769-779.

18. Leal, A.A., Et al. (2009), Interfacial behavior of high performance organic fibers. *Polymer;* 50: 1228-1235.

19. Cen, H., Et al. (2006), Micromechanics analysis of Kevlar-29 aramid fiber and epoxy resin microdroplet composite by Micro-Raman spectroscopy. *Composite Structures;* 75: 532-538.

20. Harwell, M.G., Et al. (2000), Investigation of bond strength and failure mode between SiC-coated mesophase ribbon fiber and an epoxy matrix. *Carbon;* 38: 1111-1121.

21. Herrera-Franco, P.J., and Drzal, L.T. (1992), Comparison of methods for the measurement of fiber/matrix adhesion in composites. *Composites;* 23(1):2-27.

22. Nishikawa, M., Et al. (2008), Micromechanical modeling of the microbond test to quantify the interfacial properties of fiber-reinforced composites. *International Journal of Solids and Structures;* 45: 4098-4113.

23. Lei, Z., Et al. (2008), Stress transfer of single fiber/microdroplet tensile test studied by micro-Raman spectroscopy. *Composites: Part A;* 39: 113-118.

24. Tung, N.H., Yamamoto, H., Matsuoka, T., and Fujii, T. (2004), Effect of Surface Treatment on Interfacial Strength between Bamboo Fiber and PP Resin. *JSME International Journal: Series A;* 47: 561-565.

25. Eichhorn, S.J., Et al. (2006), Analysis of interfacial micromechanics in microdroplet model composites using synchrotron microfocus X-ray diffraction. *Composites Science and Technology;* 66: 2197-2205.

26. Information about Dow Corning Brand Silicone Encapsulants. *Dow Corning®.* http://www.dowcorning.com/DataFiles/090007c88020bcca.pdf

27. Sun, L., Et al. (2010), Analysis of Interfacial Adhesion Behaviors by Single-Fiber Composite Tensile Tests and Surface Wettability Tests. *Polymer Composites;*DOI 10, 1002/pc: 1457-1464.

28. Islam, M.S. and Pickering (2007), K.L, Influence of Alkali Treatment on the Interfacial Bond Strength of Industiral Hemp Fibre Reinforced Epoxy Composites: Effect of Variation from the Ideal Stoicheometric Ratio of Epoxy Resin to Curing Agent. *Advanced Materials Research;* 29-30: 310-322.

29. Ota, T. and Matsuoka, T. (2008), Effect of post-cure condition on interfacial properties of glass fiber/vinylester composites. *High Performance Structures and Materials IV;* 129-138.

30. Silane Coupling Agents: Connecting Across Boundaries. *Gelest, Inc.* http://www.gelest.com/pdf/couplingagents.pdf

31. Wu, X. and Dzenis, Y. A. (2006), Droplet on a fiber: Geometrical shape and contact angle. *Acta Mechanica;* 185: 215-225.

32. Choi, J., Et al. (2004), Spreading of Perfluoropolyethers on FDTS-Coated Amorphous Carbon Surfaces. *IEEE Transactions on Magnetics;* 4: 3198-3191.

33. Clark, J. H. and Williamson, C. J. (1993), Mild Surface Fluorination of Glass Fibres. *Journal of Material Chemistry;* 3(6): 579-581.

Appendix A - Load Cell Calibration Data

This appendix shows the data obtained from the load cell manufacturer's calibration and calibration which was performed in the laboratory comparing with data measured by a high resolution balance (Explore Pro analytical balance from OHAUS), using standard weights of 10 – 180 mg.

Table A.1 Calibration of load cell to show its compatibility with TEDS

Test Load		Recorded Readings (mV/V)	
Applied (gf)	N	Tension	Compression
0	.0000	.00000	.00000
25	.2452	.49102	-.49105
50	.4903	.98179	-.98234
75	.7355	1.47294	-1.47374
100	.9807	1.96294	-1.96513
50	.4903	.98220	-.98254
0	.0000	.00011	-.00019

Table A.2 Calibration of the 1N load cell

Calibration Weight		Balance		Load Cell
mg	N	g	N	1 N
10	.000098	.010	.00010	.00009
20	.000196	.020	.00020	.00019
30	.000294	.030	.00030	.00028
50	.000490	.050	.00049	.00049
60	.000588	.060	.00059	.00058
70	.000686	.070	.00069	.00069
80	.000784	.080	.00079	.00078
100	.000981	.100	.00098	.00098
110	.001079	.110	.00108	.00108
120	.001177	.120	.00118	.00118
130	.001275	.130	.00128	.00128
150	.001471	.150	.00147	.00147
160	.001569	.160	.00157	.00157
170	.001667	.170	.00167	.00167
180	.001765	.180	.00177	.00177